2-17-2016

The effect of ultrasonic waves on tensile behavior of metal

Chen Ye
University of Windsor

THE EFFECT OF ULTRASONIC WAVES ON TENSILE BEHAVIOR OF METAL

By

Chen Ye

A Thesis

Submitted to the Faculty of Graduate Studies though the Department of

Mechanical, Automotive and Materials Engineering

in Partial Fulfillment of the Requirements for

the Degree of Master of Applied Science at the

University of Windsor

Windsor, Ontario, Canada

THE EFFECT OF ULTRASONIC WAVES ON TENSILE BEHAVIOR OF METAL

By

Chen Ye

APPROVED BY:

Dr. R. Rashidzadeh, Outside Program Reader
Department of Mechanical, Automotive and Materials Engineering

---

Dr. H. Hu, Department Reader
Department of Mechanical, Automotive and Materials Engineering

---

Dr. R. Riahi, Advisor
Department of Mechanical, Automotive and Materials Engineering

January 29, 2016

AUTHOR'S DECLARATION OF ORIGINALITY

I hereby certify that I am the sole author of this thesis and no part of this thesis has been published or submitted for publication.

I certify that, to the best of my knowledge, my thesis does not infringe upon anyone's copyright nor violate any proprietary rights and that any ideas, techniques, quotations, or any other material from the work of other people included in my thesis, published or otherwise, are fully acknowledged in accordance with the standard referencing practices. Furthermore, to the extent that I have included copyrighted material that surpasses the bounds of fair dealing within the meaning of the Canada Copyright Act, I certify that I have obtained a written permission from the copyright owner(s) to include such material(s) in my thesis and have included copies of such copyright clearances to my appendix.

I declare that this is a true copy of my thesis, including any final revisions, as approved by my thesis committee and the Graduate Studies office, and that this thesis has not been submitted for a higher degree to any other University or Institution.

ABSTRACT

Ultrasonic tension (with a frequency of 20 kHz and maximum output of 700W) test were performed on AA6061, AA5086, AA1100, Brass 260 and Copper 110. By comparing with simple tension test results, the ultimate tensile strength is reduced and it is found that the acoustic softening effect has influenced on formability and tensile toughness of materials. Longitudinal and transversal ultrasonic vibration has been induced to study the effect of ultrasound on the metal forming process, the two kinds of ultrasonic vibration have significant yet different effects on tensile behavior of metals in reducing the flow stress of materials and can be concluded into two different aspects: Under the application of transversal ultrasonic vibration, elongation reduces with small softening effect; When a longitudinal ultrasonic vibration is applied, the softening effect dominates and improves the strain of metals.

DEDICATION

I dedicate this thesis to my parents,

Zhigang Ye and Jing Lu,

you have successfully made me the person I am becoming,

and to my fiancée,

Meilin Yin,

for your constant source of love and encouragement during the challenges of graduate school and life.

ACKNOWLEDGEMENTS

My sincerest thanks and gratitude to Dr. R. Riahi for his supervision and valuable suggestions that guided me in this research for my M.A.Sc. at University of Windsor, to Dr. A. Edrisy for her valuable advice, constant help and encouragement in the challenging time of my research.

Sincere thanks to my committee members, Dr. H. Hu and Dr. R. Rashidzadeh, for their helpful suggestions. Sample preparation and technical support by senior technician Mr. A. Jenner is greatly acknowledged.

TABLE OF CONTENTS

LIST OF FIGURES

CHAPTER 1

CHAPTER 2

CHAPTER 3

CHAPTER 4

CHAPTER 5

LIST OF TABLES

CHAPTER 2

CHAPTER 3

CHAPTER 4

LIST OF ABBREVIATIONS

ASTM	American society for testing materials
UTS	Ultimate tensile strength
UV	Ultrasonic vibration
FE (FEM)	Finite element method
SEM	Scanning electron microscope
TEM	Transmission electron microscope
MPa	Mega Pascal
GPa	Giga Pascal
AA	Aluminum alloy

LIST OF SYMBOLS

$\boldsymbol{\sigma}$	Stress [**MPa**]
$\boldsymbol{e(e_f)}$	Strain
$\boldsymbol{P}$	Pressure [**Pa**]
$\boldsymbol{A_0}$	Original area [$\boldsymbol{m^2}$]
$\boldsymbol{\delta}$	Elongation [**mm**]
$\boldsymbol{\Delta L}$	Elongation [**mm**]
$\boldsymbol{L_0}$	Gage length of workpiece
$\boldsymbol{L_0}$	Gage length of workpiece at fracture
$\boldsymbol{s_0}$	Yield strength
$\boldsymbol{P_{(0.002)}}$	Pressure at 0.002 offset
$\boldsymbol{U_T}$	Tensile toughness [**MPa**]
$\boldsymbol{s_u}$	Ultimate tensile strength [**MPa**]
$\boldsymbol{C}$	Strength coefficient
$\boldsymbol{\dot{\varepsilon}}$	True strain rate
$\boldsymbol{c^E}$	Elastic modulus under electrical condition [**GPa**]
E	Electric field [$\boldsymbol{V \cdot m^{-1}}$]
$\boldsymbol{\beta}$	Electric displacement
$\boldsymbol{D}$	Dielectric coefficient

M	Amplification factor
$\boldsymbol{A_{large}}$	Area of larger cylindrical sections [**mm**]
$\boldsymbol{A_{small}}$	Area of smaller cylindrical sections [**mm**]
$\boldsymbol{\sigma(s)}$	Standard deviation
μ	Mathematic expectation
$\boldsymbol{x_i}$	Sample value
$\boldsymbol{N}$	Total number of samples
$\boldsymbol{I}$	Wave energy-flux density
$\boldsymbol{A}$	Amplitude [$\boldsymbol{\mu m}$]
$\boldsymbol{P}$	Average energy flow [**W**]
$\boldsymbol{\rho}$	Density of material [$\boldsymbol{Kg \cdot m^3}$]
$\boldsymbol{\omega}$	Angular velocity [$\boldsymbol{rad \cdot s^{-1}}$]
$\boldsymbol{u}$	Wave velocity [$\boldsymbol{m \cdot s^{-1}}$]
$\boldsymbol{f}$	Frequency of ultrasound [**Hz**]

Chapter 1: Introduction

1.1 Background of this Research

Forming or metal forming is the part of the metalworking process which a metal of simple form is changed through plastic deformation via metal deforming process such as rolling, forging, extrusion and drawing (schematic shown in **Figure 1.1**[1]), the workpiece is reshaped without adding or removing its composition, and its mass remains the same. Depending on kind of forming process, the failure reason for tools may vary, but the reason limiting tool life is mainly because high load of deforming force of metals, overload fracture and wear.

The initial motivation for this research is to reduce the significant cost for replacing the ruptured tool. A simple example can be seen in **Figure 1.2**[2] (a cold forged part of 19MnCr5 is taken as example), the costs for initial tooling, machine set-up and maintenance are compared with different batch sizes. However, for a extend manufacturing, the maintenance cost becomes dominant with increasing batch sizes, and the breakdown of tool maintenance largely affect the production rate.

A typical tool failure example is shown in **Figure 1.3**[2], because of the high load during metal forming process, fracture is the main reason for the breakdown of forming tools.

Because of the high tensile strength and low formability capacity, elevated

temperature metal forming is usually applied on some alloys such as high carbon steels, stainless steels and titanium alloys. However, the hot forming process affects the metal yielding behavior and eliminates the work hardening effects (**Figure 1.4**[1]) and sometimes may be undesirable. Therefore, a way to reduce material deformation load at lower temperature is needed.

1.2 Scope of this work

Ultrasonic metal forming is one of options applied on metal forming processes mentioned above for the purpose of decreasing forming force and therefore less tool wear and better production rate. In this research, two sets of apparatuses were used to investigate plastic deforming behavior of 5 kinds of materials.

Typical and ultrasonic tension tests were performed, quantitative analysis of ultrasonic metal forming process is still unrealizable due to the lack of experimental method and many disagreements of fundamental mechanisms of vibrated plastic forming. This work depicts comprehensive analysis of macroscopic tensile behavior of 5 metals under two kind of ultrasonic vibration conditions.

1.3 Objective of Research

In this study, the objective is to discover the underlying effect of ultrasonic vibration on plastic deformation of AA1100, AA5086, AA6061, Copper 110 and brass 260.

Determine the effect of longitudinal and transversal ultrasonic vibration on tensile strength and elongation of the above mentioned materials.

1.4 Organization of this Thesis.

This thesis is consists of 6 chapters. The contents of each chapter have been described as below:

Chapter 1 is the introductory chapter describing the background and objective of this research.

Chapter 2 shows the insight of previous studies related to ultrasonic vibration tension test. It starts with the initial innovative research by Blaha and Langenecker who proposed the “Blaha effect” and begin the interest of this area. The content following covers the representative studies and experimental method for the purpose of mechanism discovery.

Chapter 3 exhibits the experimental procedure and apparatus, and sample preparation used in this research also shown in this section.

Chapter 4 provides the results, showing the effect of ultrasonic tension test, by comparing with static tension test, the stress reduction and changes in strain are the most important. The difference between two sets of apparatus is also provided in this section.

Chapter 5 discusses the results of chapter 4, beginning with quantitative analysis of difference between transversal and longitudinal ultrasonic vibration, and following with energy prospective concern of this study. The effect of ultrasonic vibration is analyzed in this section.

Chapter 6 summarizes the entire research and presents the conclusions of ultrasonic tension test studied, including a suggestion of future work in this field of research.

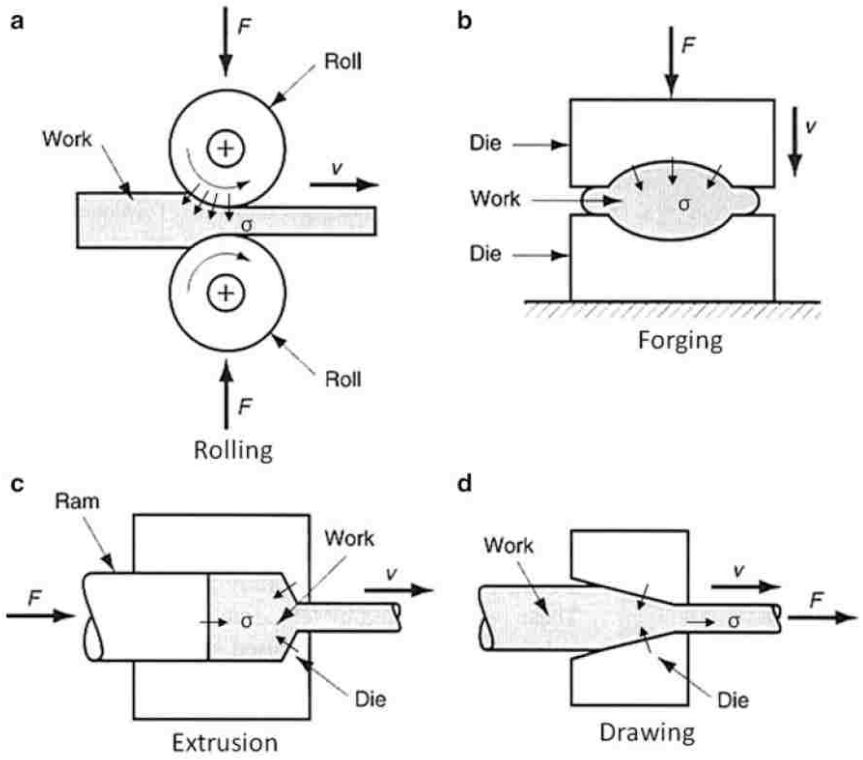

Figure 1.1[1] Illustration on the applied force and primary stress state in (a) rolling, (b) forging, (c) extrusion, and (d) drawing.

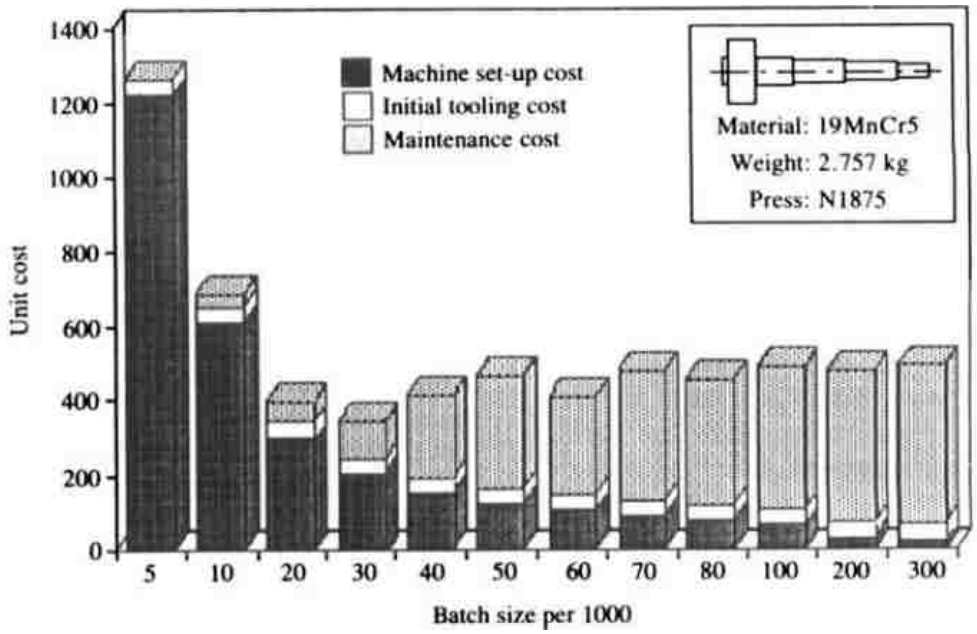

Figure 1.2[2] Initial tooling cost, machine set-up cost and maintenance cost for a typical cold forged part.

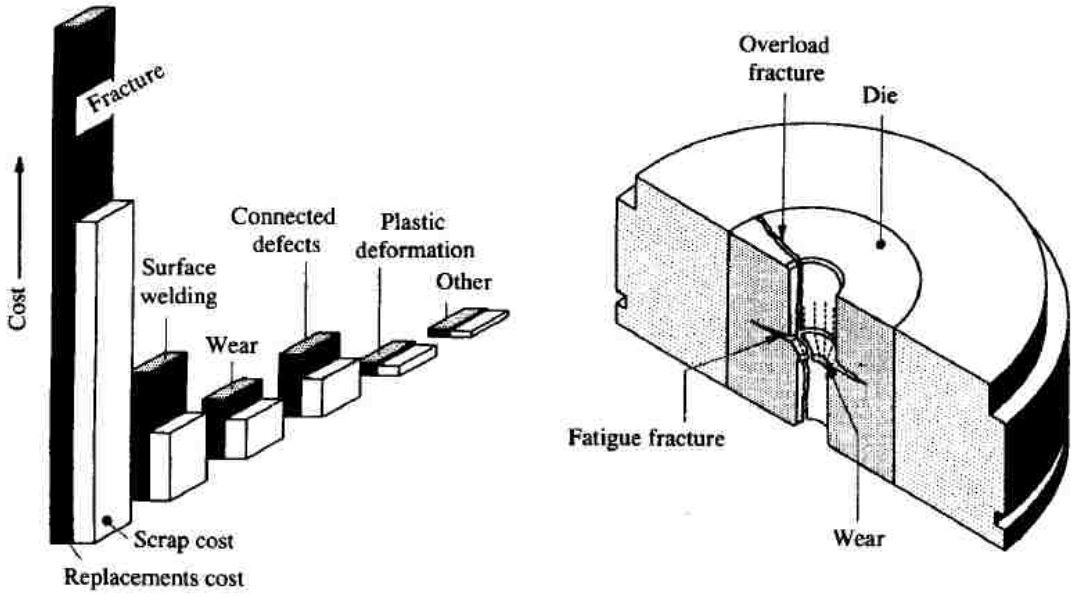

Figure 1.3[2] Typical tool failures in cold extrusion

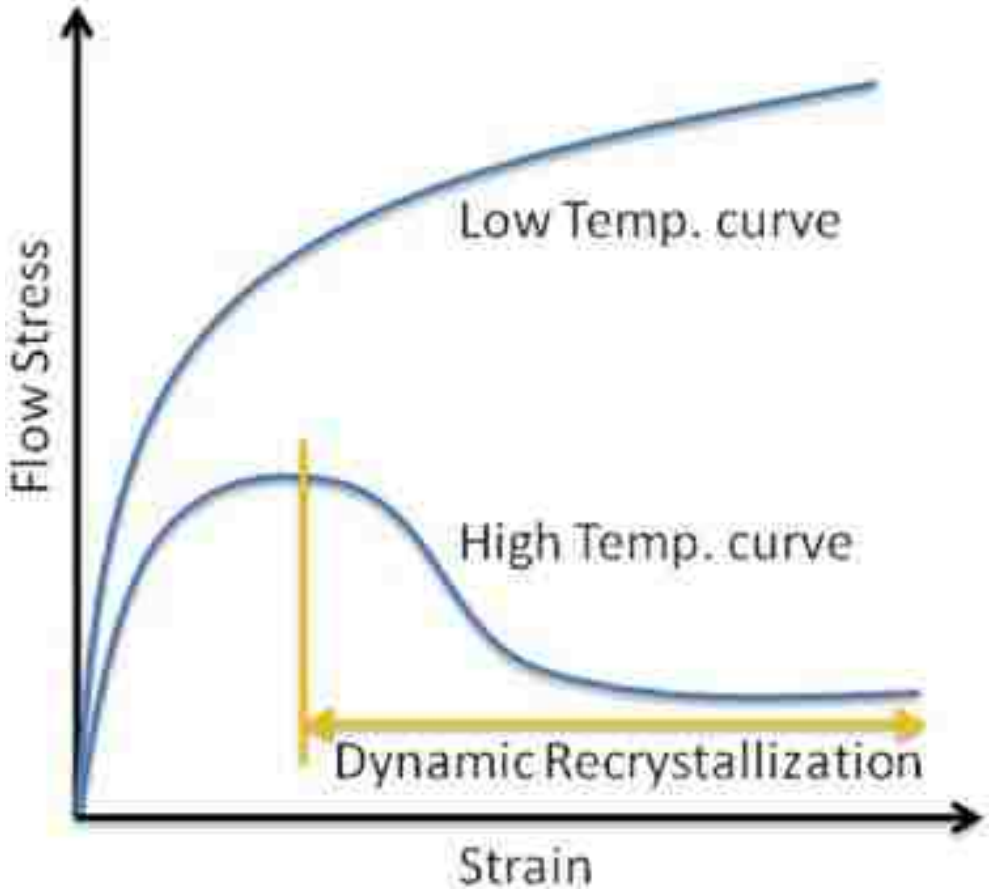

Figure 1.4[1] The effect of dynamic recrystallization on the metal flow

Chapter 2: Literature Survey

2.1 Introduction to this survey

There are many parameters affecting the tensile behavior of materials, for static tension test, strain rate and temperature are well recognized to affect materials' tensile strength. While in ultrasonic tension test, besides strain rate and testing temperature, the universal mechanism can be applied on both low and high-frequency remains unclear. This survey explains the previous important and innovative research on ultrasonic tension tests, metal forming mechanisms and their experimental apparatus are introduced in this section.

2.2 Static tensile test of ductile metals

Tension (tensile) test is the general way to obtain mechanical properties of metal, in which represents the process of standard workpieces resisting external axial forces until they fractured. In the meantime, the data obtained from tension test can be plotted as stress-strain curve indicating the maximum elongation (strain) and tensile stress (including ultimate tension strength).

Figure 2.1 shows a typical stress-strain curve for ductile metal such as magnesium[3]. OA represents the initial elastic deformation stage obeying Hooke's law, Point A is the maximum elastic limit, it also representing the maximum load which workpiece can bear

without having permanent deformation when load is removed. Point A' is the proportional limit, which representing the starting point that a stress-strain curve is no longer linear (end of elastic deformation).

It's easily concluded that with the conformability of Hooke's law [3], at elastic region of stress- strain curve, the slope of stress-stain curve is a approximately linear according to each material representing the modulus of elasticity, or Young's modulus. Giving the value of,

$$\frac{\boldsymbol{\sigma}}{\boldsymbol{e}} = \mathbf{E} = \mathbf{constant} \qquad (2\text{-}1)$$

Point B is called the yield strength, defined as the external force that will produce permanent deformation, often approximately 0.002 of strain (0.2%). At last, the offset OC is the strain that plastic deformation happened. As the workpiece elongated, the resistance of workpiece (internal force) becomes stronger. As a result, the load reaches its maximum with increasing elongation. In the end, necking happened on the workpiece and the diameter of material decreased rapidly until the workpiece failed.

2.3 Static tensile test of brittle metals

For brittle metal, such as cast iron, only a small plastic deformation region shows after it reaches the UTS. This phenomenon show the importance of material ductility, because it allows material distribute the concentrated stress when external load outreaches maximum, and transform this localized stresses into self-strain. The

completely brittle material and brittle material stress-strain behavior are shown in **Figure 2.2 (a)(b)**[3].

2.4 Important parameters in engineering tension test

2.4.1 Engineering stress, strain and toughness

The stress used in this thesis is the average longitudinal stress [3] in tensile workpiece, calculated and obtained by using the load divided by original area of the cross section of the standard workpeices followed by ASTM E8/E9 [4].

$$\mathbf{s} = \frac{\boldsymbol{P}}{\boldsymbol{A_0}} \tag{2-2}$$

The average longitudinal stress is also called engineering stress and is simply referred as stress in the following statement.

The strain used for the stress-strain curve is the average linear strain [3] (conventional strain), obtained by dividing the elongation of the gage length of the workpiece ,

$$\mathbf{e} = \frac{\boldsymbol{\delta}}{\boldsymbol{L_0}} = \frac{\boldsymbol{\Delta L}}{\boldsymbol{L}} = \frac{\boldsymbol{L - L_0}}{\boldsymbol{L_0}} \tag{2-3}$$

The engineering stress-strain curve will have the same form as load-elongation curve since both average stress and conventional strain are obtained by dividing a constant. The engineering stress-strain curve can be seen from **Figure 2.3**[3].

The yield strength is another important parameter which represents the stress needed to have an initial stage of plastic deformation. The common parameter to define this stress is by using the stress of 0.002 offset strain divided by the original cross section of

the workpiece[3].

$$s_0 = \frac{P_{(strain\ offset=0.002)}}{A_0} \tag{2-4}$$

The tensile toughness of a material is the ability to absorb energy (external energy) in the plastic range. The higher absorption of external energy is desirable for many parts in manufacturing, such as bearing materials, gears and couplings, to withstand abnormal external stress conditions, especially above its yield stress.

Tensile toughness is determined by the total area under the stress-strain curve. The mathematical value of this area represents the amount of work per unit volume the material can absorb without causing it fail. **Figure 2.4**[3] shows the typical stress-strain curve for high and low tensile toughness workpieces.

As shown in **Figure 2.4**[3], the high-carbon steel (similar with cast iron) has higher yield strength yet lower elongation. On the other hand, the structural steel has higher ductility and better extension. As a result, the total area of structural steel is far greater than high-carbon steel and indicates structural steel is tougher than high-carbon steel. Higher yield strength of high-carbon steel makes it more resilience. By calculating the mathematical area under the curve, the tensile toughness can be presented precisely, and several mathematical approximations can also made to predict tensile toughness qualitatively [3].

$$U_T \approx s_u e_f \tag{2-5}$$

and

$$U_T \approx \frac{s_0 + s_u}{2} e_f \tag{2-6}$$

Where s_u is ultimate tensile strength, and s_0 represents yield strength at 0.002 offset and e_f for elongation.

2.4.2 Comparison with true stress-strain curve

The biggest difference between true stress and engineering stress (stress) is original cross sectional area (A_0) has been used entirely for the calculation of stress. As a matter of fact, the cross sectional area changes constantly with elongation happened. Therefore, by using the actual cross sectional area, the plastic deformation stage in true stress-strain curve exhibits different pattern with engineering stress strain curve for the cross sectional area keep decreasing in this stage.

The true stress should be obtained from actual necking cross sectional area in the tension test [3],

$$\sigma = \frac{P}{A} \tag{2-7}$$

Therefore, the true strain should also be changed due to instantaneous gage length, determined by,

$$\varepsilon = \sum \frac{L_1 - L_0}{L_0} + \frac{L_2 - L_2}{L_1} + \frac{L_3 - L_2}{L_2} + \cdots \tag{2-8}$$

or

$$\varepsilon = \ln(e + 1) \tag{2-9}$$

Figure 2.5 [3]compares the true stress-strain curve and engineering stress-strain curve. As can be seen from **Eq (2-7), (2-9)**, the true stress-strain curve is at the left of strain

curve.

Some of the diagram in the following statement use true stress-strain curve to represent the effectiveness of ultrasonic vibration.

2.4.3 Effect of strain rate on material stress

The strain rate is usually defined as the rate of deformation carried out and is conventionally expressed in the units of $\boldsymbol{s^{-1}}$, per second, the range of strain rates is given in **Table 2.1[3].**

The typical effects of temperature and strain rate can be seen from **Figure 2.6[5]**, noted that with the modulus elasticity usually increased along with temperature, the tensile strain becomes more sensitive with the change of strain rate. As **Figure 2.6** indicates, the basic relationship between stress and strain rate at certain temperature is,

$$\boldsymbol{\sigma = C(\dot{\varepsilon})^m|_{\varepsilon,T}} \tag{2-13}$$

where C is the strength coefficient and $\dot{\boldsymbol{\varepsilon}}$ is the true strain rate (true strain per unit time), m is the strain-rate sensitivity and can be obtained from the slop of log $\boldsymbol{\sigma}$ vs log$\dot{\boldsymbol{\varepsilon}}$.

2.5 Power ultrasonic transducers: principles and design

2.5.1 The basic mechanism of piezoelectric materials

The ability of certain material to transform high frequency electrical fields into mechanical displacement is the basic of the construction of ultrasonic transducer. This

effect is called piezoelectric effect and first found by Curie brothers in 1880s, the basic schematic is illustrated in **Figure 2.7[6].**

Aligned electric dipoles exist within the material creates the effect of piezoelectric. In order to produce the tensile stress, a charge on the faces of the ceramic is needed (means a voltage across the piezoelectric ceramic material), and the separation of dipoles is the trigger of this phenomenon.

A modified Hooke's law[6] can be used in scenario,

$$\boldsymbol{\sigma = c^E \varepsilon} \tag{2-10}$$

Where $\boldsymbol{\sigma}$ is stress, $\boldsymbol{\varepsilon}$ is strain, and $\boldsymbol{c^E}$ is the elastic modulus. The superscript represents its measurement under electrical condition. As a result, a similar expression can be described by,

$$\boldsymbol{E = \beta D} \tag{2-11}$$

Where E is electric field, D is the electric displacement and $\boldsymbol{\beta}$ represents the dielectric coefficient.

2.5.2 The design of power ultrasonic transducer

A simple power ultrasonic transducer is shown in **Figure 2.8[6]**. With only one side of voltage charged, piezoelectric disks should be placed on opposite direction (left and right side). Electrodes made of steel are spaced between piezoelectric materials.

Several considerations should be noticed while using ultrasonic transducer:

- Heat production. Heat will be produced during the use of ultrasonic transducer due to the losses in ceramics and metals. Various cooling methods or interval between tests should be conducted.
- Vibration amplitude. If a higher vibration amplitude is desired, a relatively low mass material is often used at the front (such as aluminum or titanium) and use heavy metal at the back (such as steel, it can help to create “mass” amplification).
- “Shape” amplification can be achieved by using smaller diameter front mass compared with bigger diameter back front.
- Assembly. Bolted transducer will need flats or spanner holes in the front of transducer.
- Fixture. For the purpose of forcing transducer against load, the ultrasonic transducer must be tightly held at testing point.

A common power ultrasonic transducer is shown in **Figure 2.9**[6], an external and internal view can be seen clearly, the steel back mass and front mass support the transducer and make the piezoelectric ceramic material less likely damaged.

2.5.3 The ultrasonic horns

In order to focus the ultrasonic waves at a small area or volume (e.g. ultrasonic metal forming), an ultrasonic horn is usually installed to achieve the goal. For a stepped horn,

the amplification factor is given by the areas of two cylindrical sections[6],

$$M = A_{large}/A_{small} \quad (2\text{-}12)$$

The horn is half-wavelength long, and a node is located along the axis of the horn. **Figure 2.10**[6] shows typical stepped horn and tapered horn.

2.6 Ultrasonic metal deforming and its mechanisms

Plastic deformation is the main character of metal forming processes (e.g. rolling, forging, extrusion and drawing, shown in **Figure 1.1**[1]) after which material deformed and reshaped into ideal geometry, the applied force must exceed the yield strength of metal material. Ultrasonic metal forming is a technique by applying ultrasonic vibration on these metal forming processes in order to achieving less tool wear, increasing production speed and mainly decreased forming forces.

2.6.1 Metal deforming behavior in ultrasonic tension test

The very first and most well-known experiment came from a short note by Blaha and Langenecker in 1955 and it draw both interest and controversy of researchers among the world rapidly[7-12]. **Figure 2.12**[13] shows the ultrasonic tension result from early Langenecker work. Line A of Figure 2.12 (a) shows the significant drop in force of single crystal Zinc with the aid of ultrasonic vibration (800kHz). Line B indicates the effect for continuous ultrasonic vibration. Since this is the first report commenting the effect of

ultrasonic vibration on metal deforming process, no clear mechanism was proposed in the first time note, but the contribution of this first note for latter author is critical [14-18].

Another very typical ultrasonic tension test example was carried out by Tong Wen[19], who uses AZ31 magnesium alloy and adjustable ultrasonic transducer. Both apparatus and experiment have been very innovative, moreover, softening and hardening effects have been observed under different power of ultrasonic transducer in this research. Modified ultrasonic generator and workpiece can be seen in **Figure 2.13**[19], ultrasonic vibration in this research is adjustable from 20%A to 90%A (A is maximum amplitude, A=0.003mm), "Hardening" effect and "Softening" effect are respectively representing the reduction of strain and increase in strain in this study. As can be seen in **Figure 2.14**[19], lower ultrasonic (20%-50%) excitation tends to increase the elongation of AZ21 while under high ultrasonic excitation of 60%-90%, the elongation was decreased and means the "hardening" effect becomes more dominant.

No matter what ultrasonic vibration used, high or low, the immediate drop of stress of AZ31 has been observed in this research (**Figure 2.15**[19]). All ultrasonic tension tests show lower yield strength than static tension test (**Figure 2.14**).

2.6.2 Metal deforming behavior in ultrasonic upsetting and compression test

In 2012, Yao et al. showed an improved ultrasonic compression test system (shown

in **Figure 2.16**[20]). Barreling effects and surface roughness were measured, one of the most innovation idea of this research is that past single-cause mechanism (ultrasonic wave superposition, softening effect or surface effect) may not be able to explain the reduction of flow stress entirely, coupled mechanisms should be considered (mainly acoustic softening and stress superposition) to predict the real mechanism of stress reduction effect.

The combination of effects is:

- Stress superposition.
- Acoustic softening.
- Friction decrease.

The most important resource of reduction is from acoustic softening and stress superposition shown in **Figure 2.17**[20], this conclusion well explained the outcome of previous research [21-24].

2.6.3 The effect of oscillatory stress superposition on ultrasonic metal forming

The oscillatory stress superposition theory is still remained an analytical model rather than more detail quantitative calculation on ultrasonic metal forming, the principle of stress superposition was first founded by Kirchner [25] for low frequency. **Figure 2.18 (b)** [25] shows the path of maximum oscillatory stress with parallel but lower than static stress

(**Figure 2.18 (a)** [25]). In Kirchner's study, the analytical model was well confirmed for low frequency experiments and therefore provides excellent theoretical foundation for latter development.

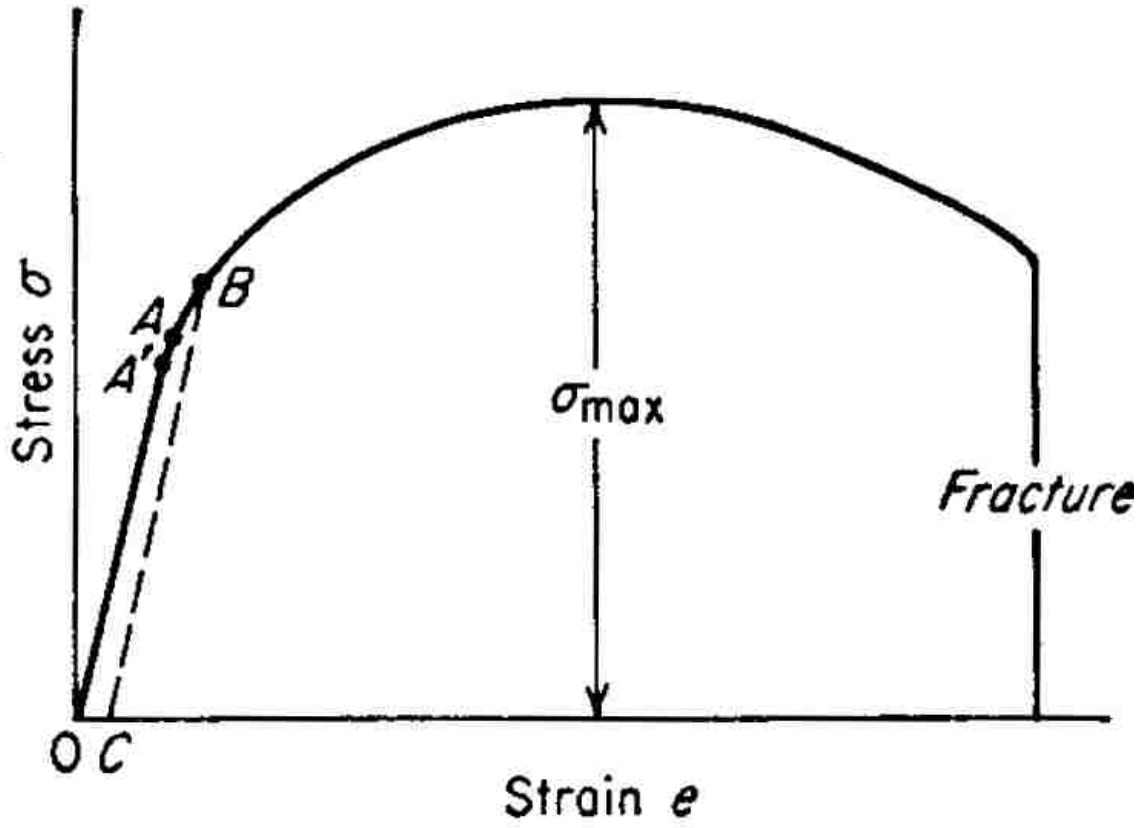

Figure 2.1[3] Typical tension stress-strain curve.

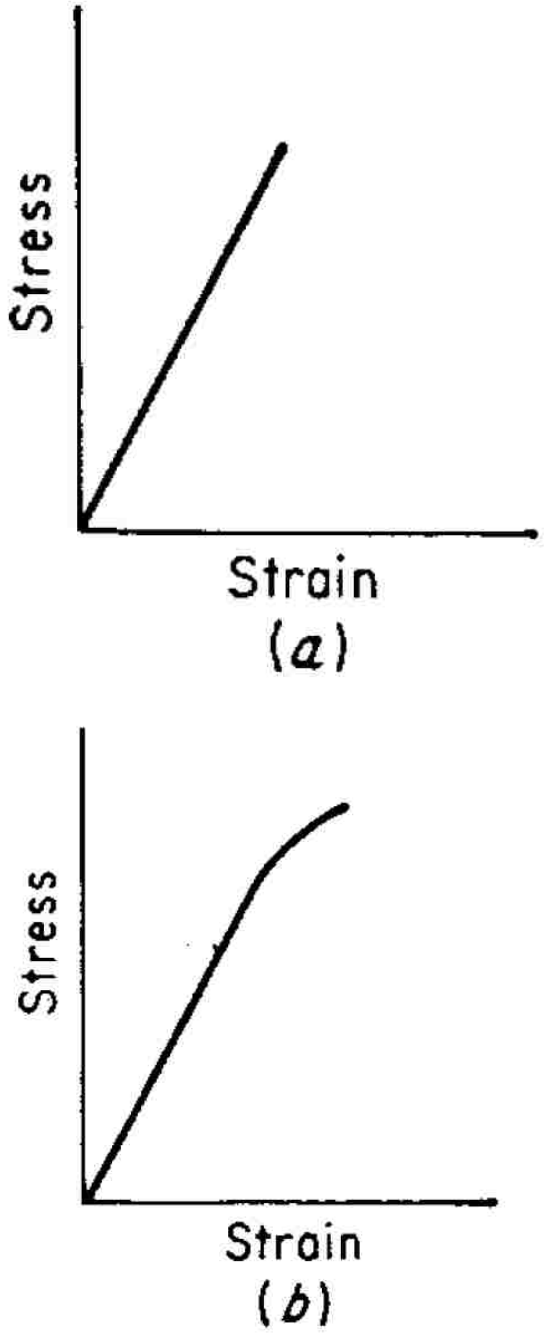

Figure 2.2[3] (a) Stress-strain curve for completely brittle material (ideal behavior); (b) stress-strain curve for brittle metal with slight amount of ductility.

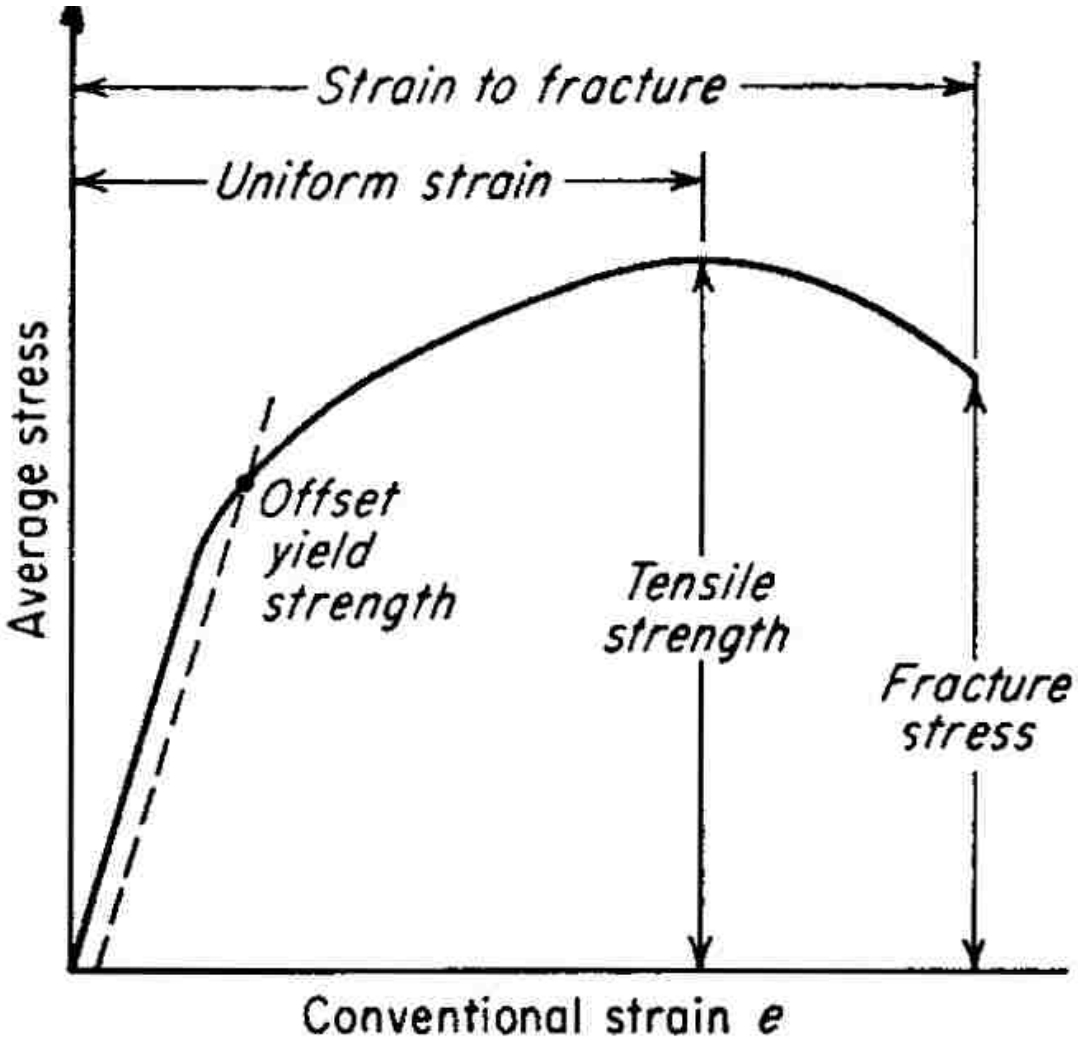

Figure 2.3[3] The engineering stress-strain curve.

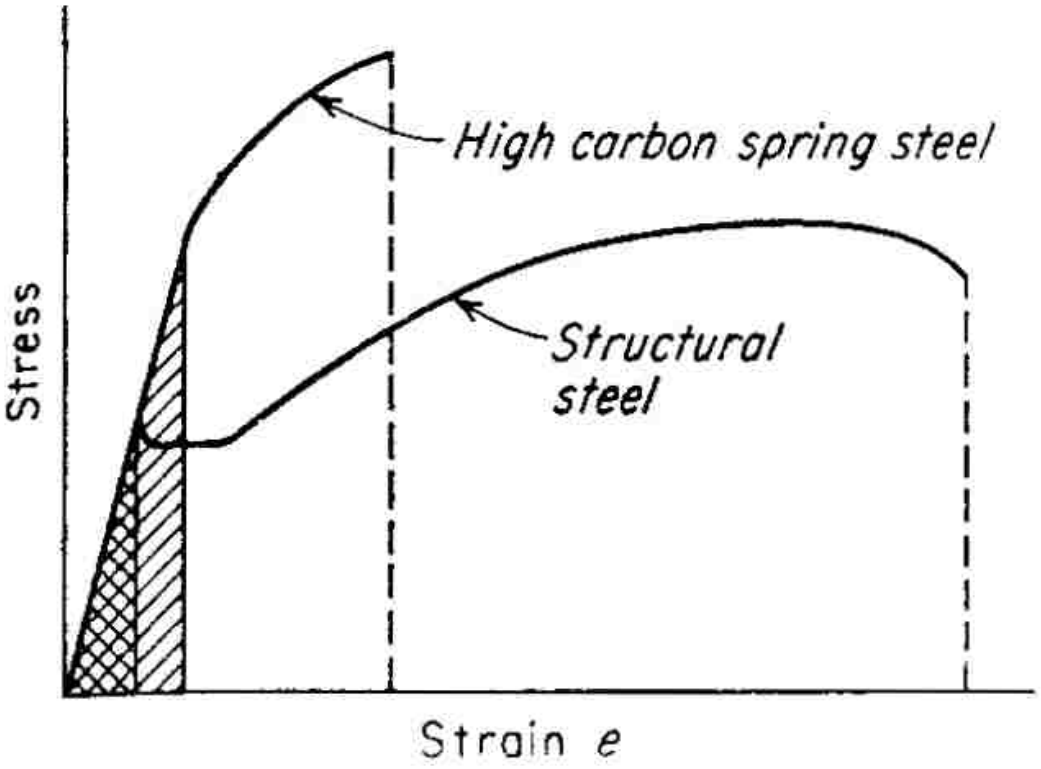

Figure 2.4[3] Comparison of stress-strain curves for high and low-toughness materials.

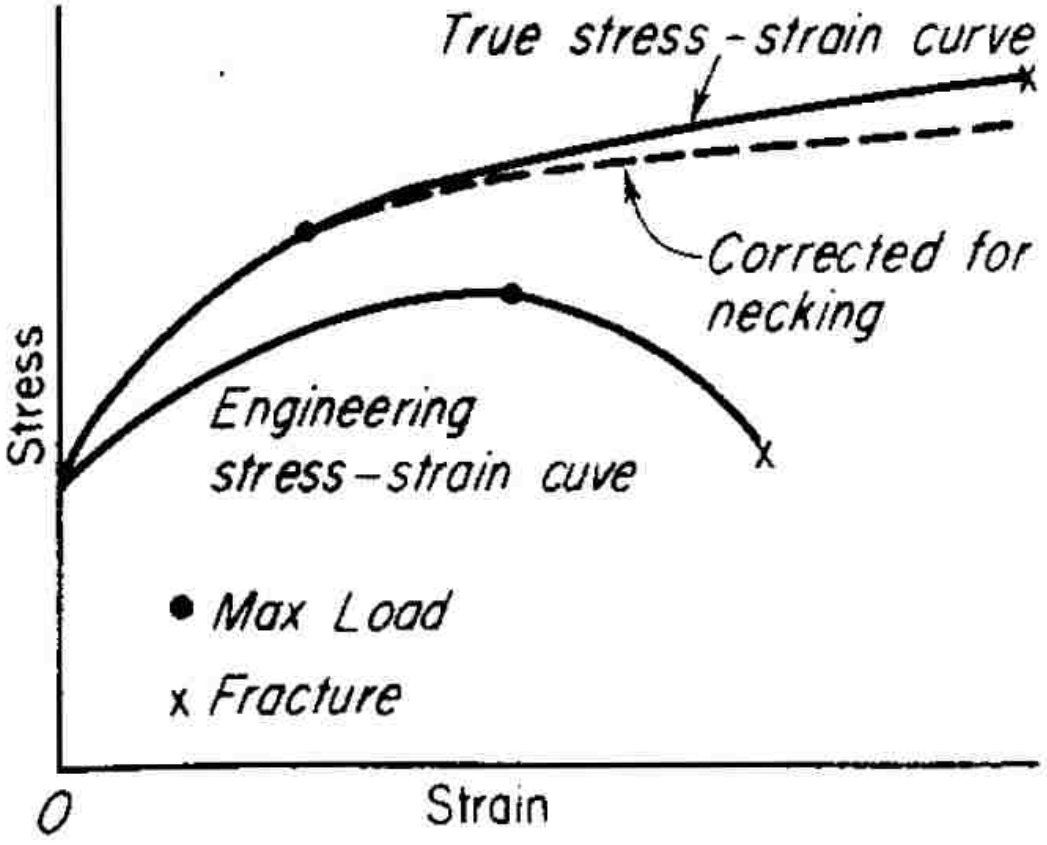

Figure 2.5[3] Comparison between engineering curve and true stress-stain curve

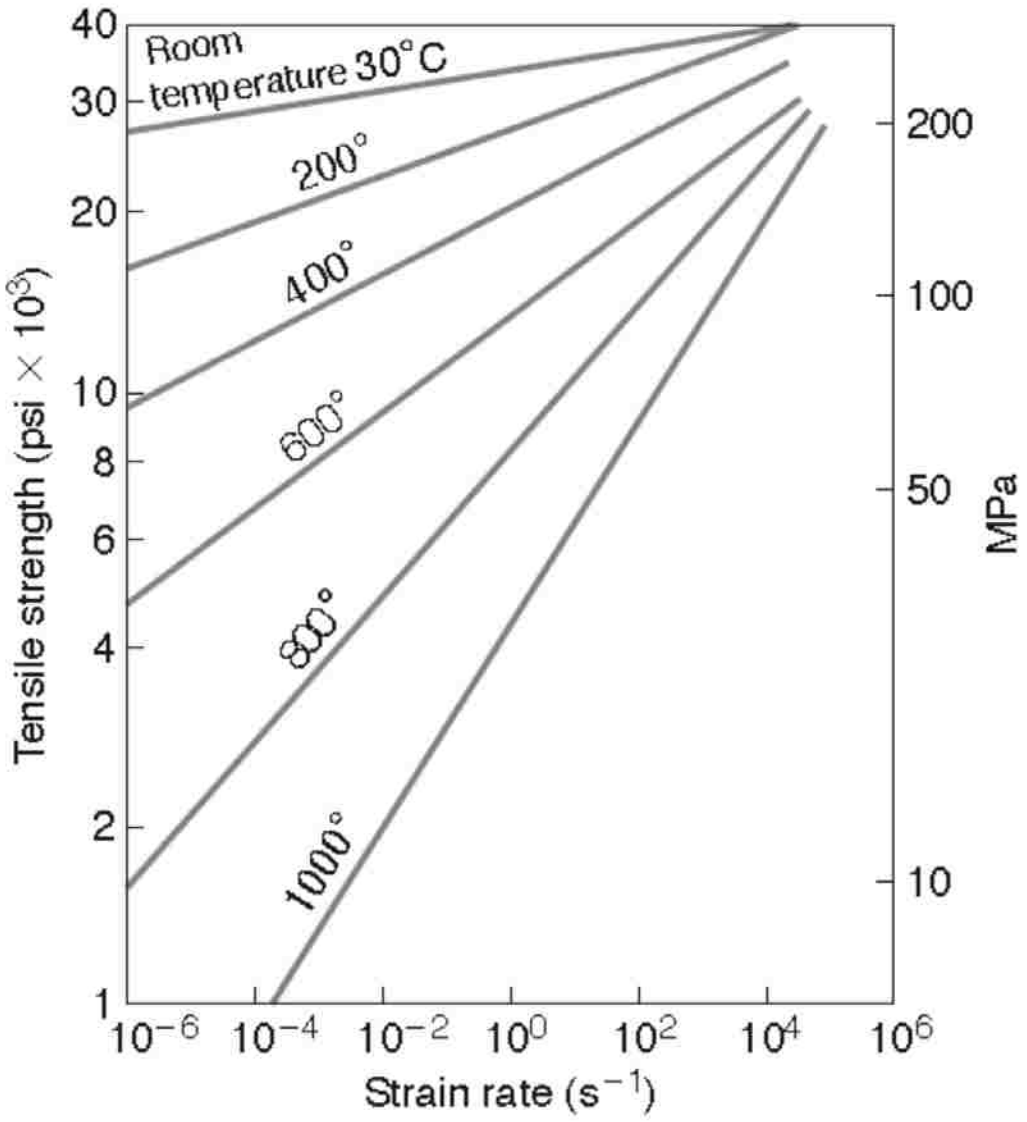

Figure 2.6[5] The effect of strain rate on the ultimate tensile strength for aluminum. Note that, as the temperature increases, the slopes of the curves increase.

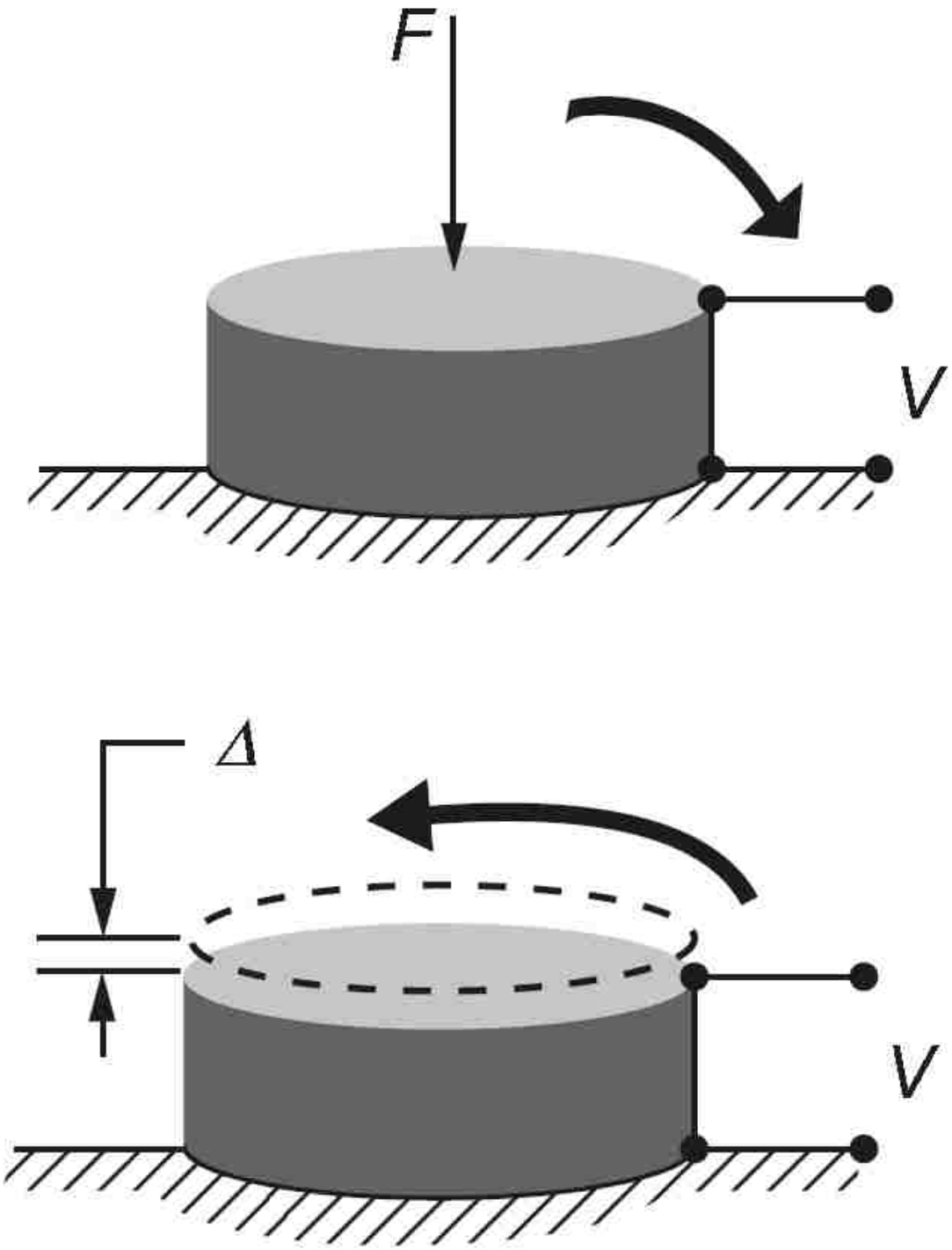

Figure 2.7[6] Piezoelectric effect: Direct (top) and inverse (bottom).

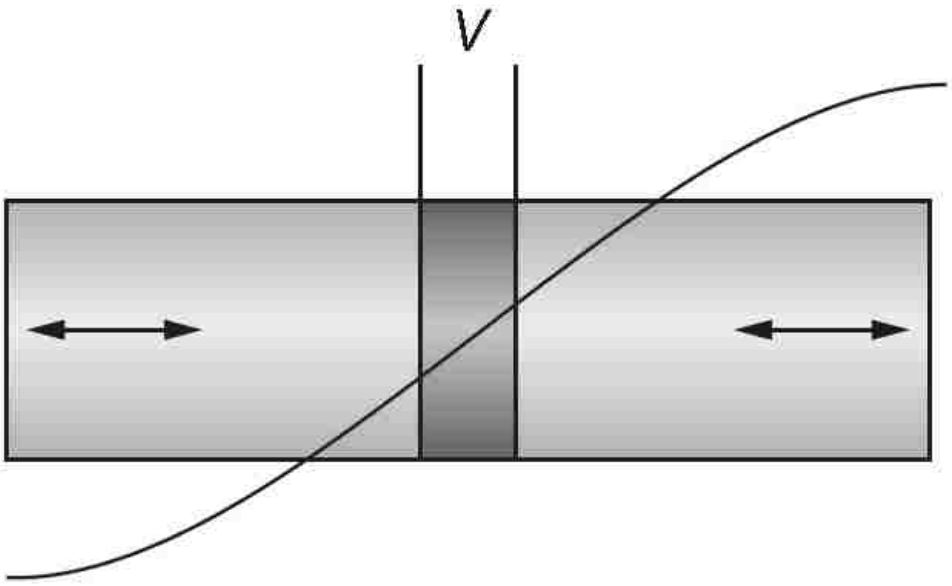

Figure 2.8[6] Basic power ultrasonic transducer.

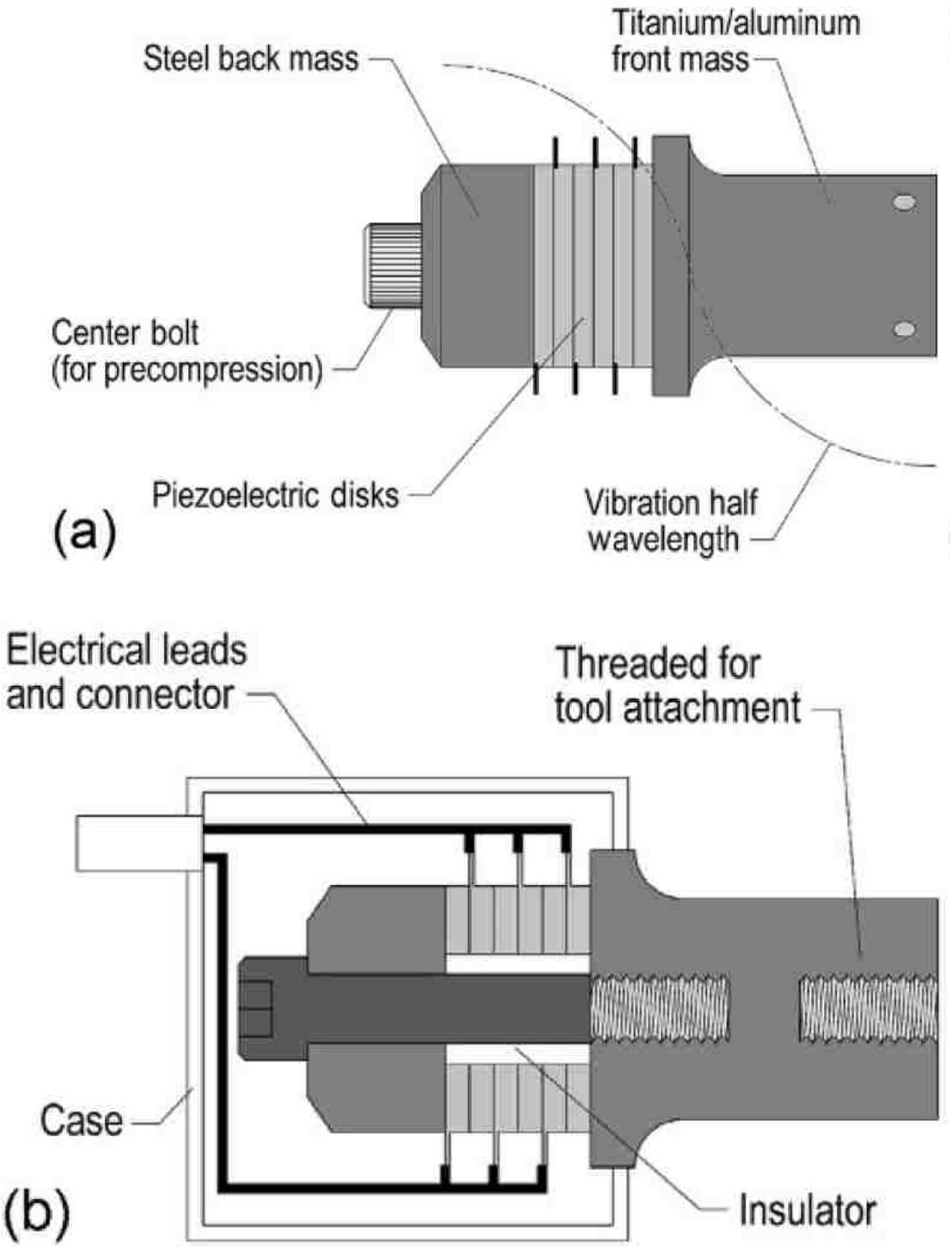

Figure 2.9[6] Representative power ultrasonic transducer: (a) external view; (b) internal view.

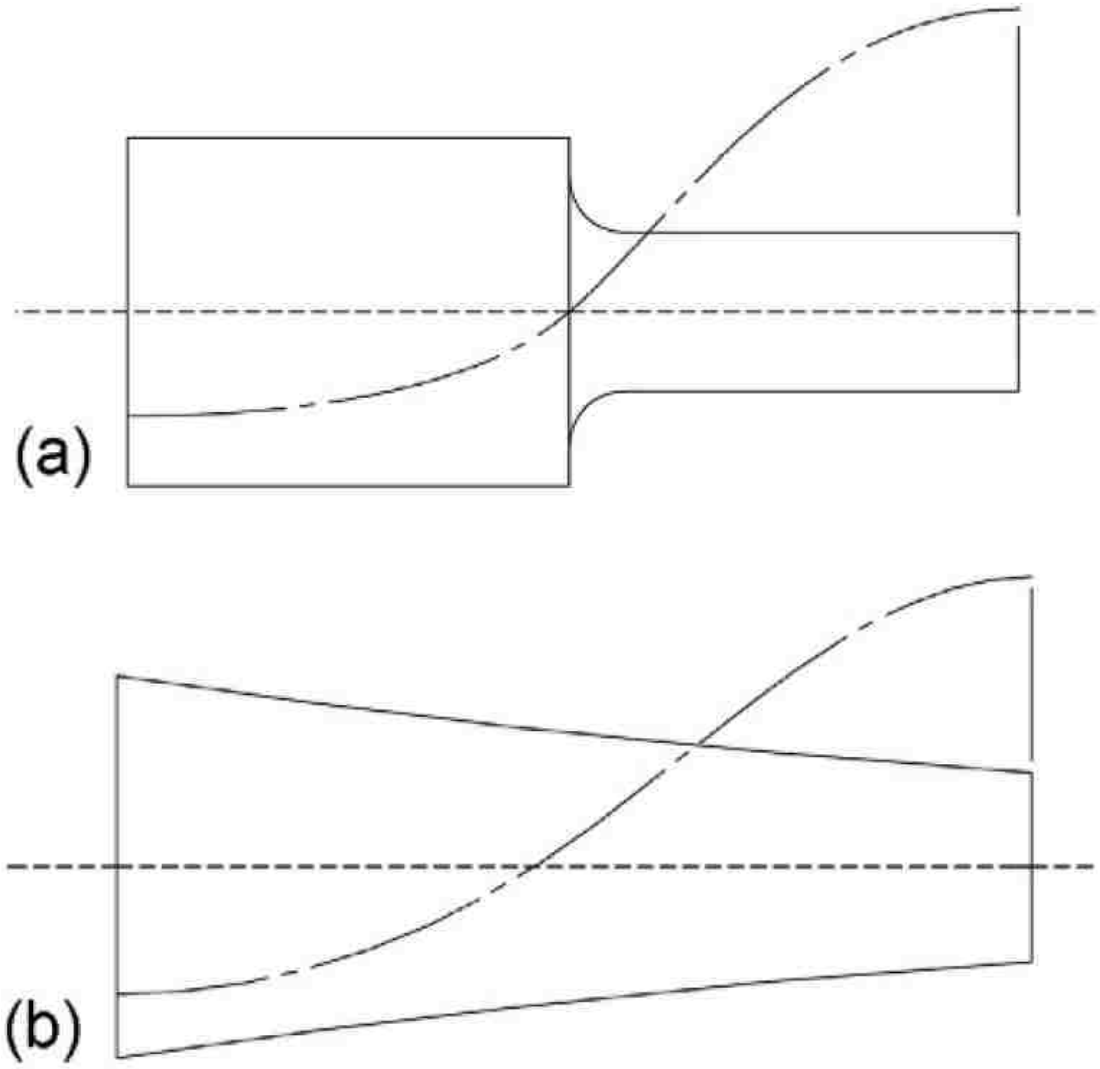

Figure 2.10[6] Ultrasonic horns: (a) stepped horn; (b) tapered horn.

Table 2.1[3] Range of strain rate

Range of strain rate	Condition or type test
10^{-8} to 10^{-5} s^{-1}	Creep tests at constant load or stress
10^{-5} to 10^{-1} s^{-1}	"Static" tension tests with hydraulic or screw-driven machines
10^{-1} to 10^{2} s^{-1}	Dynamic tension or compression tests
10^{2} to 10^{4} s^{-1}	High-speed testing using impact bars (must consider wave propagation effects)
10^{4} to 10^{8} s^{-1}	Hypervelocity impact using gas guns or explosively driven projectiles (shock-wave propagation)

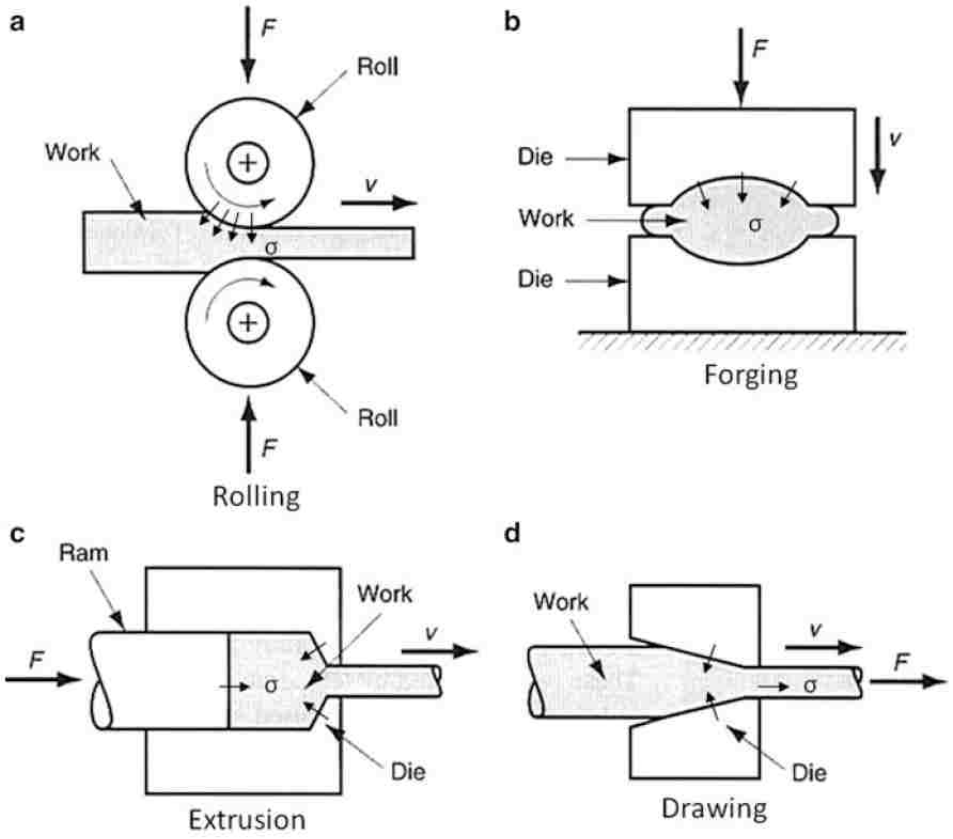

Figure 2.11[1] Illustration on the applied force and primary stress state in (a) rolling, (b) forging, (c) extrusion, and (d) drawing.

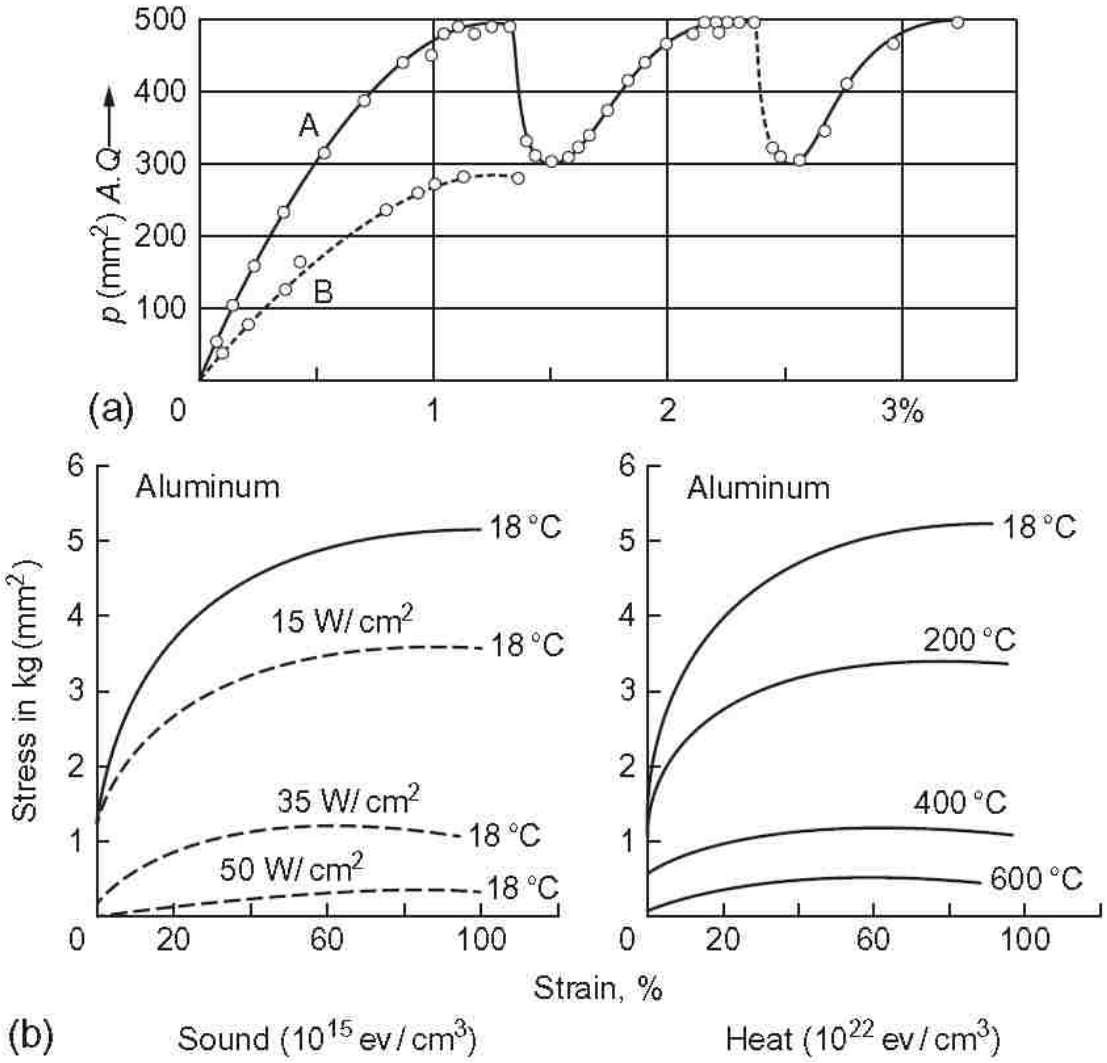

Figure 2.12[13] (a) Effect of ultrasound on the force-deformation of zinc (Blaha and Langenecker, 1955); (b) equivalence of ultrasound treatment to increased temperature (Langenecker, 1963).

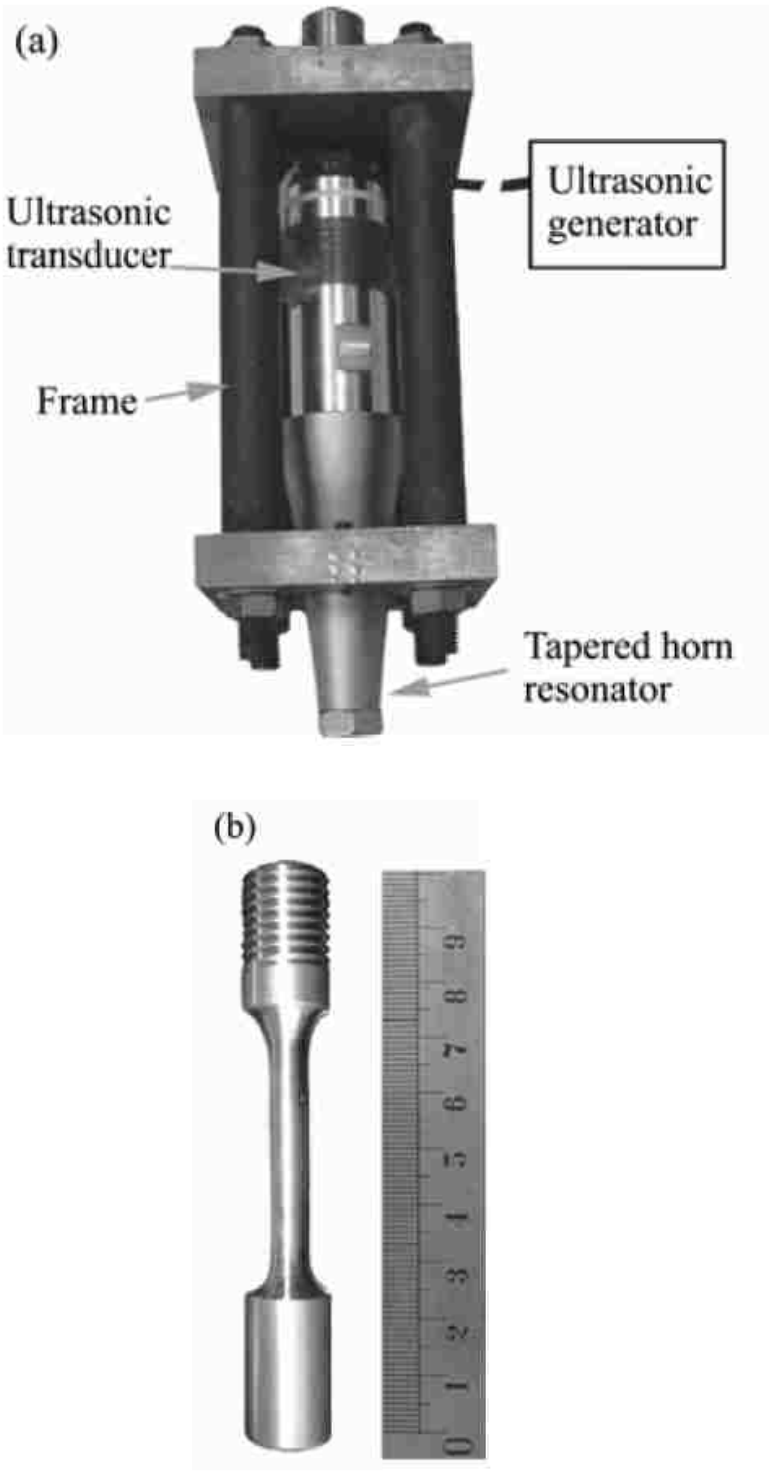

Figure 2.13[19] Ultrasonic-vibration apparatus (a) and AZ31 sample for tensile testing (b).

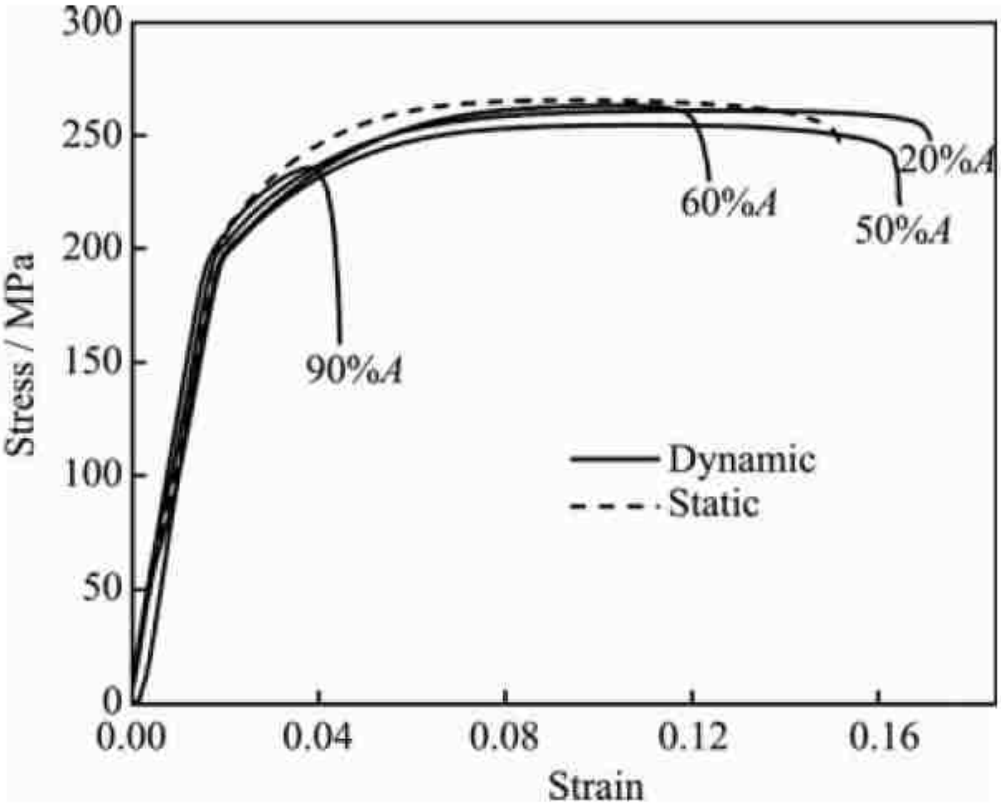

Figure 2.14[19] Stress-strain curves of AZ31 under static tension and vibrated tension with different amplitudes.

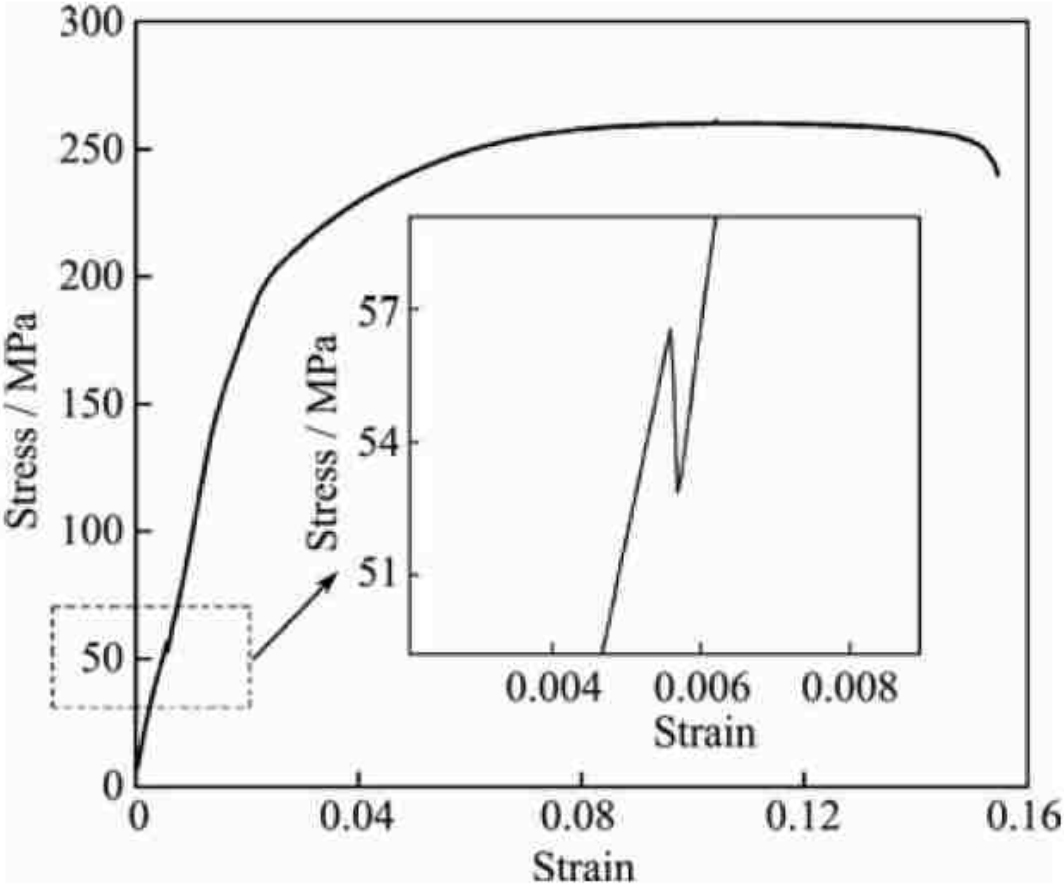

Figure 2.15[19] Decrease of flow stress at the ultrasonic vibration amplitude of 20%A.

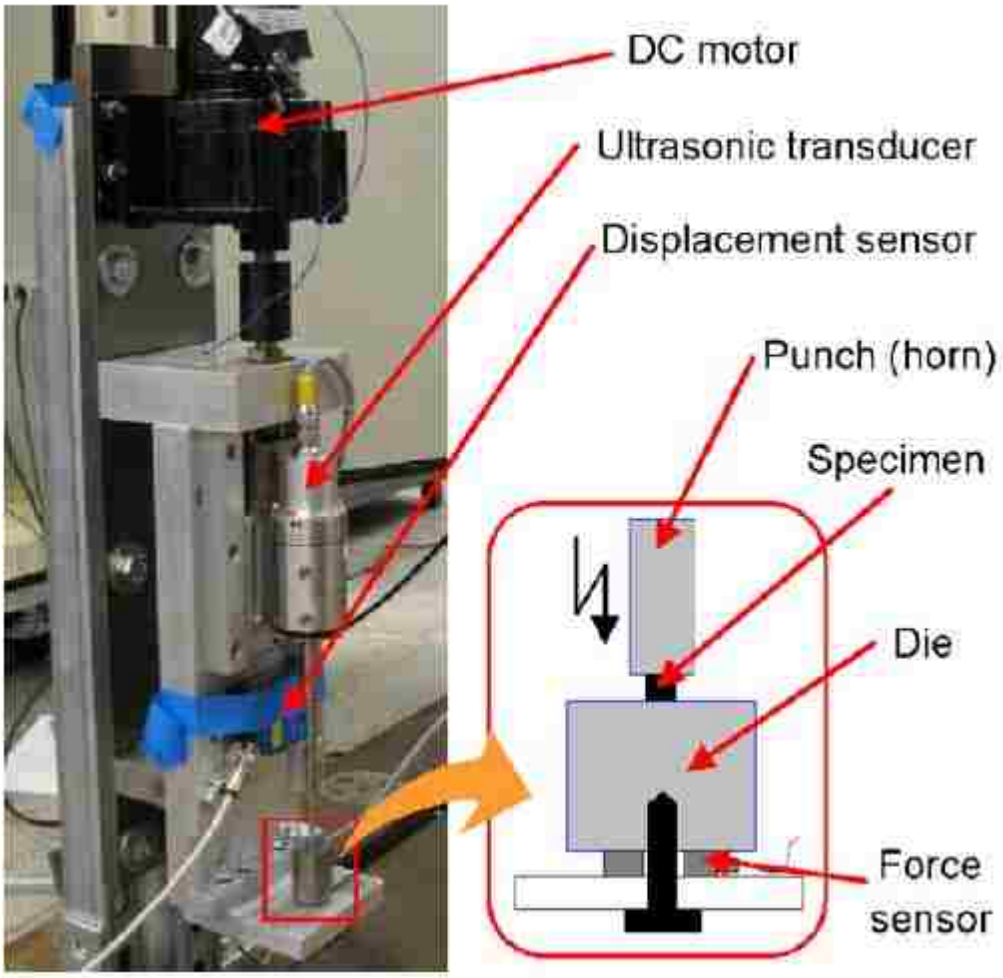

Figure 2.16[20] Improved experimental setup for vibration-assisted micro/meso upsetting.

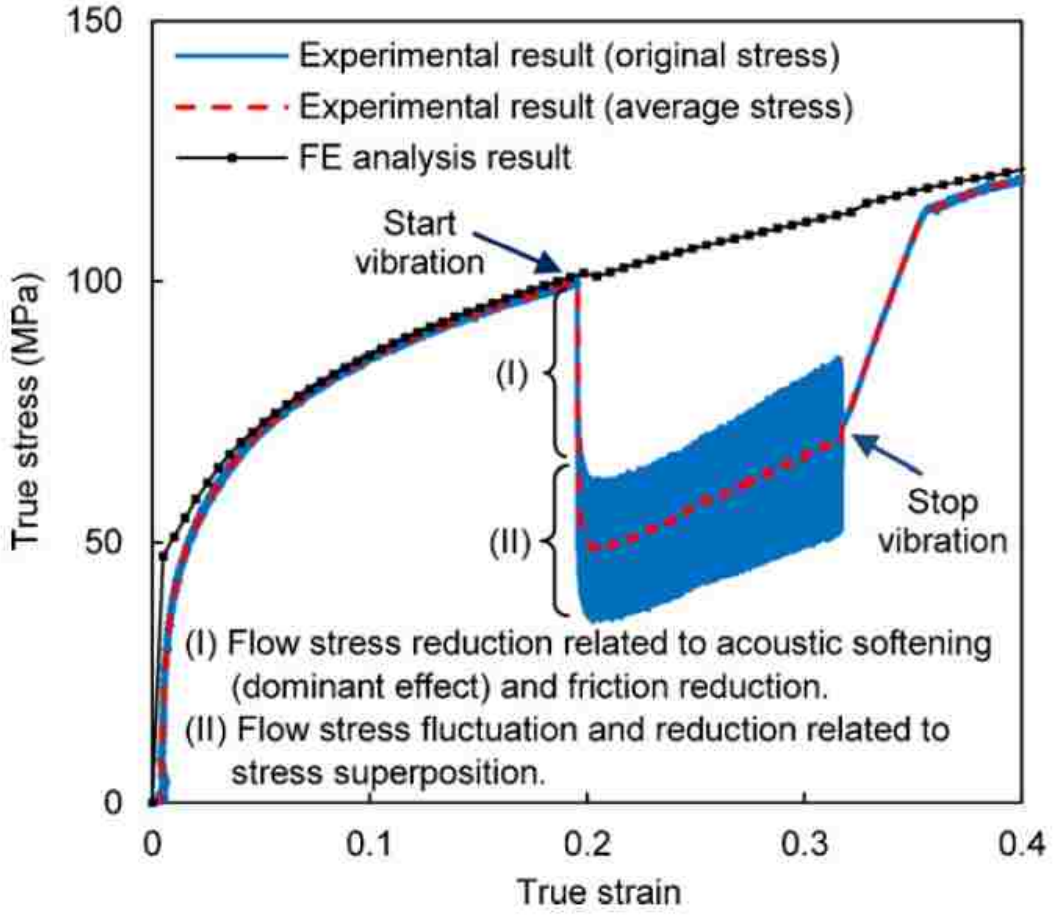

Figure 2.17[20] Comparison of true stress–strain curves of the micro/meso upsetting from experiment and FE analysis.

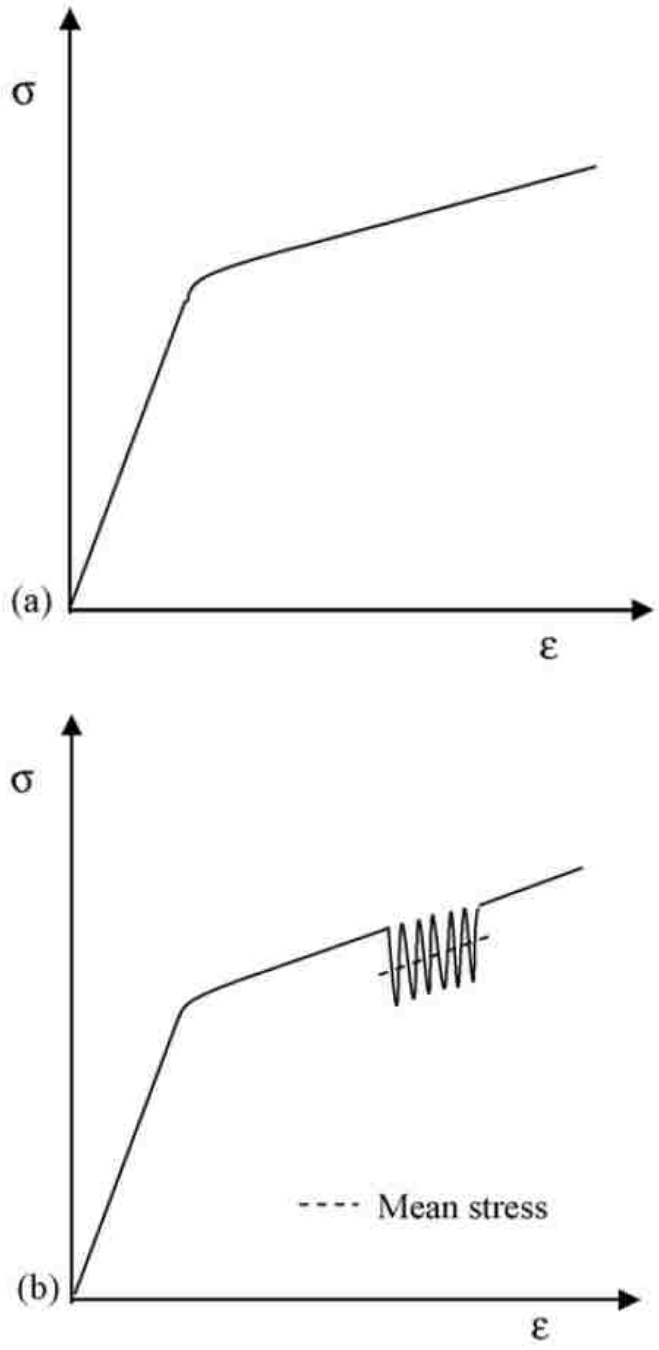

Figure 2.18[25] (a) Static stress–strain curve for an elastic–plastic material and the principle of oscillatory stress superposition effect shown in (b).

Chapter 3: Experimental

3.1 Description and Preparation of Workpieces

3.1.1 Aluminum 6061 alloy

Aluminum 6061 is one of the most widely used and popular choices for vehicle parts and pipe fittings. It has better corrosion resistance and weldability than AA2024 and AA7075. AA6061 with following composition (in wt%) shown in **Table 3.1** was studied. The as-received T6 tempered grade AA6061 has a thinness of $\mathbf{0.063}$" with thickness tolerance of $\pm\mathbf{0.004}$" and meets the AMS 4027.

According to ASTM E8/E8M-09[4], all metallic materials for tension testing must have specific dimension as guided, especially the gage length, according to E8/E8M, the minimum gage length for tension test is 25mm and the maximum up to 50mm, the dimension of standard workpiece for tension test is as shown in **Table 3.2**. The machined workpiece and its dimension are shown in **Figure 3.1** and **3.2.** Some practical changes have been applied on the workpieces due to the apparatus used in this study: 1. The gage length is adjusted to $\mathbf{36}\boldsymbol{mm} \pm \mathbf{1}\boldsymbol{mm}$ in order to fit between preinstalled fixture and standard grip; 2. Only one side of grip section is saved so that can guarantee the sufficient grip force of the fixture. The component of the ultrasonic tension system is discussed in 3.3.

3.1.2 Aluminum 5086 alloy

Aluminum 5086 alloy offers excellent corrosion resistance with good formability. It is not usually strengthened by heat treatment, so AA5086 can be easily welded and retain most of its mechanical strength. The composition of AA5086 studied in this research is shown in **Table 3.3**. The thickness is $\mathbf{0.063}''$ with thickness tolerance of $\pm\mathbf{0.004}$". The sample was annealed before testing, the equipment for heat treatment is shown in **Figure 3.3**.

3.1.3 Aluminum 1100 alloy

1100 aluminum alloy is an aluminum-based alloy and treated as commercially pure wrought aluminum, usually can be strengthened by cold working, not by heat treatment. It has good electrical conductivity and high corrosion resistance. The composition of AA1100 studied is shown in **Table 3.3**. The as-received AA1100 is at $\mathbf{1/2}$ hard condition and meets ASTM B209 and tempered grade is H14. The sample was annealed before testing.

3.1.4 Brass 260

Brass 260 alloy is a kind of high formability copper alloy mainly with combination of copper and zinc, it provides good corrosion resistance but not as machinable as 300 series brass. The composition of brass 260 studied in this research is shown in **Table 3.4**, the material is in $\mathbf{1/2}$ hard condition and meets ASTM B36. The thickness of material is

$\mathbf{0.063}$" and with thickness tolerance of $\pm\mathbf{0.006}$". The sample was annealed before testing

3.1.5 Copper 110

Copper 110 offers high electrical conductivity and 99.90% purity, and it often used in electrical application, such as wire connectors. It can be soldered and brazed, and received in $^{\mathbf{1}}/_{\mathbf{2}}$ hard condition. The sample was annealed before testing, and the composition can be seen in **Table 3.5**).

3.2 Static and Ultrasonic tension test

Static and ultrasonic tension tests were performed by using a Instron tension tester (**Figure 3.4**)(model: TTD) on AA6061, AA5086, AA1100, Brass 260 and Copper 110. Tension test for each material was performed under room temperature (25℃) and repeated five times. The strain rate of $\mathbf{1.46 \times 10^{-3} s^{-1}}$ was used for static and ultrasonic tension tests.

3.3 Apparatus of ultrasonic tension test

In previous studies, longitudinal vibration has been adopted for most experiments[26-28], few reports concentrate on the transverse vibration. In this work, one of the innovative ideas is to compare the effect of longitudinal and transverse ultrasonic

vibration. The contributive mechanism induced by both ultrasonic directions was analyzed as well.

In order to perform the ultrasonic tension test on both vibration directions, a system which can easily transform between two vibration directions is of great importance. Four components were used to consist the system: 1. Ultrasonic transducer (A); 2. Workpiece fixture (B); 3. Transducer holder for longitudinal tension test system (C); and 4. Transducer holder for transversal tension test system (D). The schematic show of components are shown in **Figure 3.5**.

The ultrasonic generator used in this research is produced by JiaYuanDa Technology (model no. JYD-2000). The working frequency is 20kHz and output power of ultrasonic transducer is 700W.

3.3.1 Transversal ultrasonic tension system

The transversal ultrasonic tension system can be assembled by component (A), (B) and (D), and shown in **Figure 3.6.** When ultrasonic vibration is imposed, a pre-installed moveable joint (highlighted with red square) can guarantee the freedom of ultrasonic vibration.

3.3.2 Longitudinal ultrasonic tension system

The longitudinal ultrasonic tension system is assembled by component (A), (B) and (C). The schematic show for the system can be found in **Figure 3.7**, which ultrasonic

transducer has been turned 90° and installed in longitudinal holder.

Table 3.1 Composition of AA6061 (wt%)

Element (wt %)	Si	Fe	Cu	Mg	Cr	Ni
Composition	0.4-0.8	0-0.7	0.05-0.4	0-0.15	0.4-0.8	0-0.05
Element (wt %)	Zn	Ti	Zr	Other	Al	
Composition	0-0.25	0-0.15	0.025	0.15	95.1-98.2	

Table 3.2 Composition of AA5086 (wt%)

Element (wt %)	Si	Fe	Cu	Mg	Cr	Zn
Composition	0-0.4	0-0.7	0-0.1	0.2-0.7	0.05-0.25	0.25
Element (wt %)	Ti	Other	Al			
Composition	0.15	0.15	93-95.7			

Table 3.3 Composition of AA1100 (wt%)

Element (wt %)	Si	Cu	Mn	Mg	Zn	Ti
Composition	0.55-1.0	0.05-0.2	0-0.05	0-0.05	0-0.1	0-0.6
Element (wt %)	other	Al				
Composition	0-0.15	97.85-99.4				

Table 3.4 Composition of Brass 260 (wt%)

Element (wt %)	Cu	Zn	Fe	Pb
Composition	68.75-71.5	26.38-31.38	0-0.05	0-0.07

Table 3.5 Composition of Copper 110 (wt%)

Element (wt %)	Cu	Pb	Bi	O
Composition	99.9	0-0.005	0-0.005	0-0.04

Table 3.6[4] Standard dimension of ASTM E8/E8M, selected dimension used in workpieces.

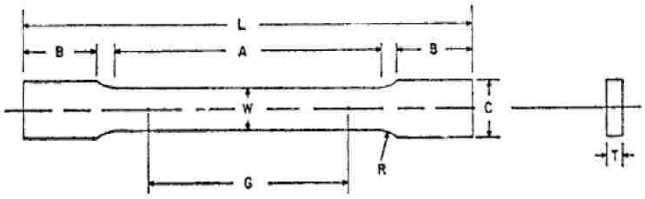

	Dimensions		
	Standard Specimens		Subsize Specimen
	Plate-Type, 40 mm [1.500 in.] Wide	Sheet-Type, 12.5 mm [0.500 in.] Wide	6 mm [0.250 in.] Wide
	mm [in.]	mm [in.]	mm [in.]
G—Gage length	200.0 ± 0.2 [8.00 ± 0.01]	50.0 ± 0.1 [2.000 ± 0.005]	25.0 ± 0.1 [1.000 ± 0.003]
W—Width	40.0 ± 2.0 [1.500 ± 0.125, -0.250]	12.5 ± 0.2 [0.500 ± 0.010]	6.0 ± 0.1 [0.250 ± 0.005]
T—Thickness		thickness of material	
R—Radius of fillet, min	25 [1]	12.5 [0.500]	6 [0.250]
L—Overall length, min	450 [18]	200 [8]	100 [4]
A—Length of reduced section, min	225 [9]	57 [2.25]	32 [1.25]
B—Length of grip section, min	75 [3]	50 [2]	30 [1.25]
C—Width of grip section, approximate	50 [2]	20 [0.750]	10 [0.375]

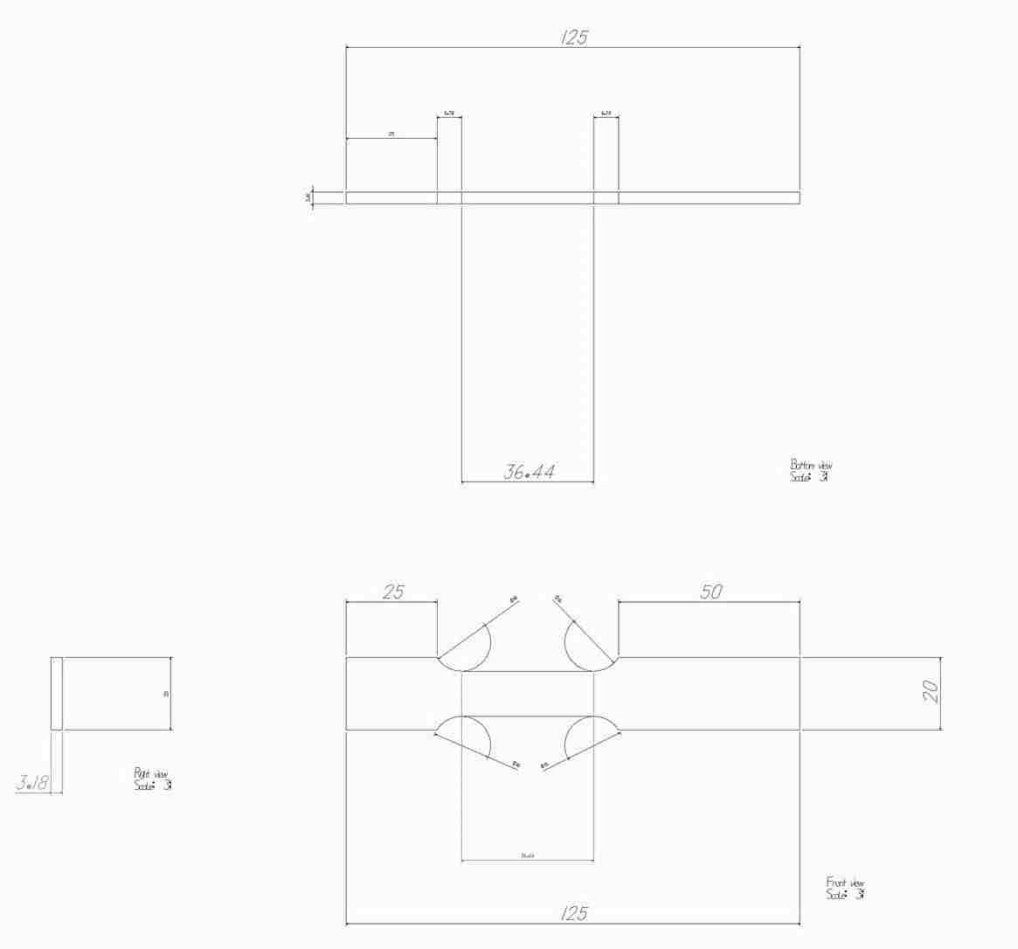

Figure 3.1 Dimensions of workpiece, unit: mm.

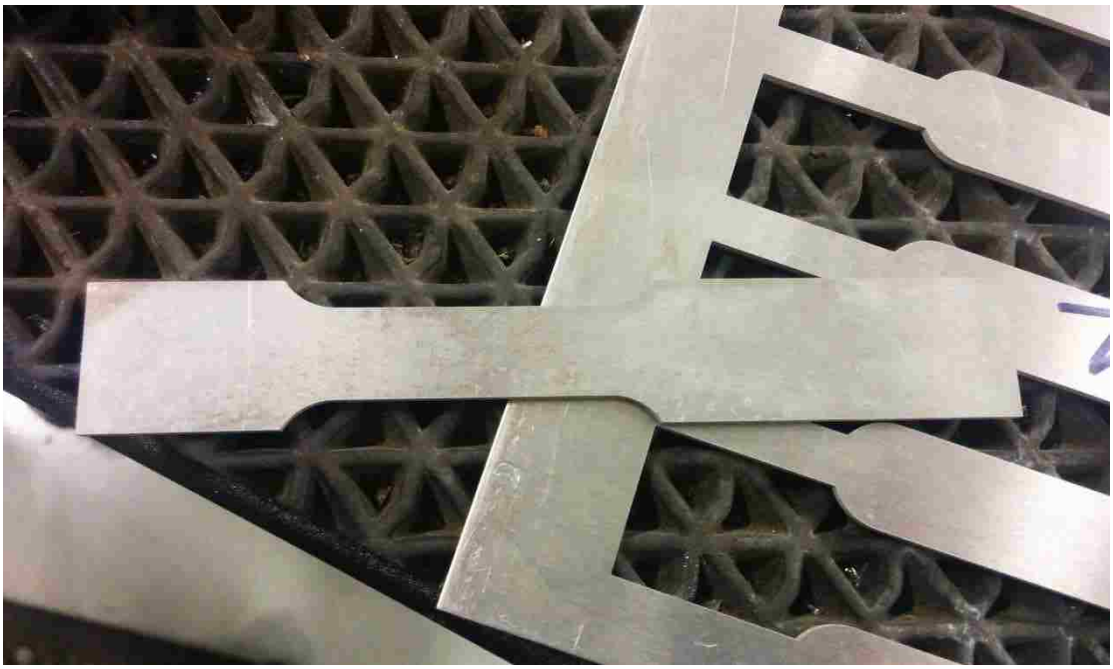

Figure 3.2 Machined standard workpiece for ultrasonic tension test.

Figure 3.3 Furnace for heat treatment.

Figure 3.4 Tension tester manufactured by Instron Universal Testing Instrument.

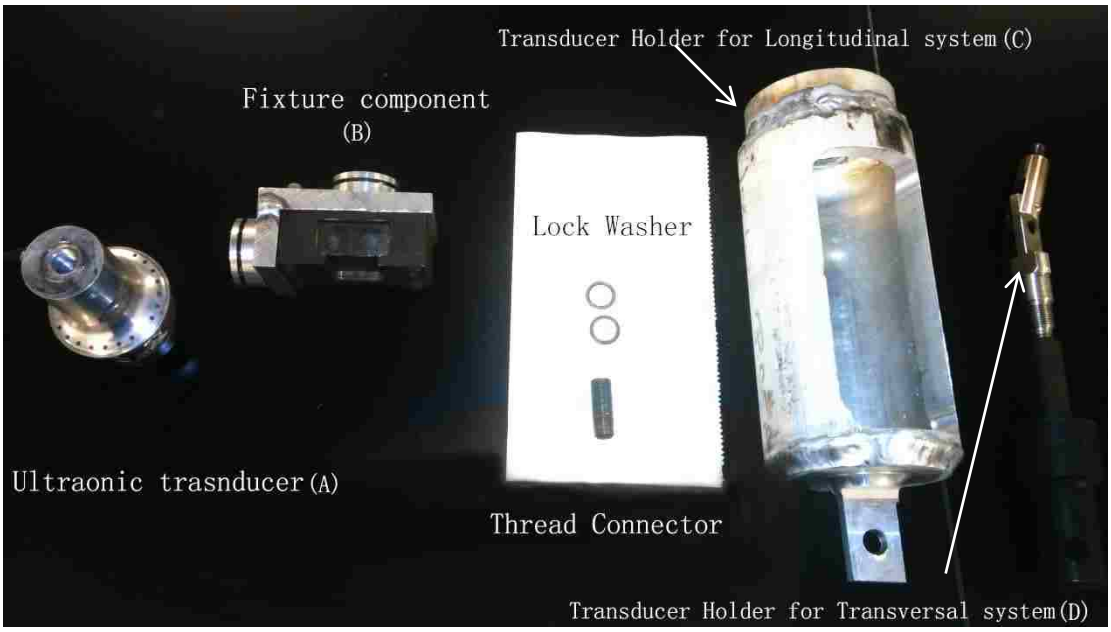

Figure 3.5 Four components consisting ultrasonic tension system.

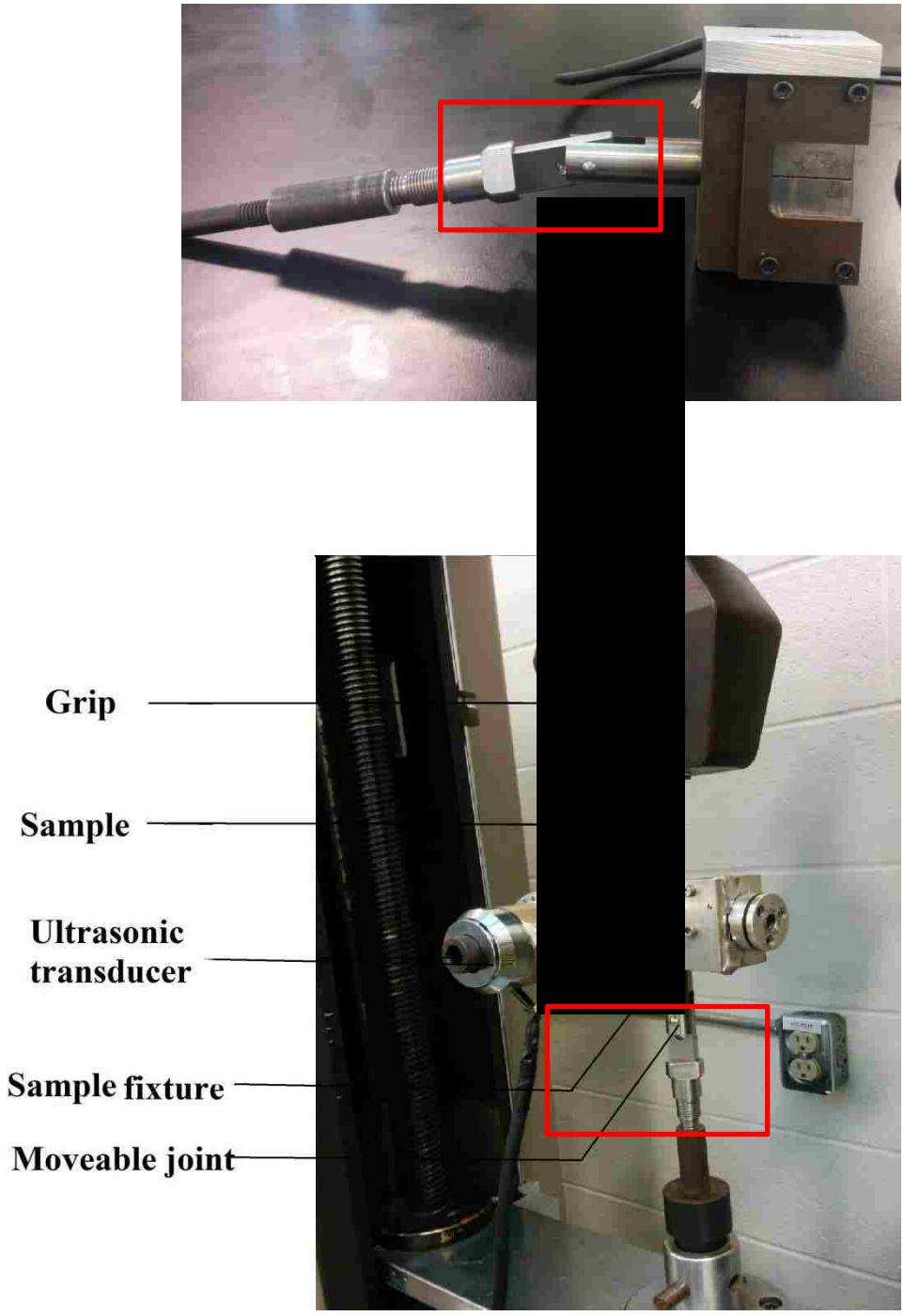

Figure 3.6 Transversal ultrasonic tension system.

Figure 3.7 Longitudinal ultrasonic tension system.

Chapter 4: Results

4.1 Ultrasonic vibration tension results of AA6061

Figure 4.1 shows the stress-strain curves of AA6061 under static tension and ultrasonic vibration with transverse direction. Five species were tested for each vibration condition. The reduction in elongation and small softening effect exists in ultrasonic tension test after the superimposition of vibration. This effect is also found from other materials observed by Blaha and Langenekcer[29]. Because the difference between the apparatus and power of ultrasonic transducer used in this study, the stress reduction is not as much as Langnecker reported. However, the stress reduction phenomenon validates the mechanism of acoustic softening and effect of ultrasonic vibration. In the tests, the resistance of the deformation of all AA6061 workpieces was decreased as soon as the ultrasonic vibration was imposed and stress started to bounce back immediately after stopping the vibration (shown in **Figure 4.2**).

Elongation stands for the formability of one specific material. As can be seen in Figure 4.1, the elongation of AA6061 decreases at certain ultrasonic vibration energy, but also the deformation resistance of AA6061 declined. This means under 700W input power of ultrasonic transducer, AA6061 are more likely to be deformed than in non-ultrasonic condition.

Figure 4.3 shows stress-strain curves of AA6061 under static tension and ultrasonic vibration with longitudinal direction. There existed so-called “softening effect” (increase in elongation/strain) in ultrasonic tension test after the superimposition of vibration. Similar with transversal tension test, as soon as longitudinal ultrasonic vibration was excited, the stress of AA6061 in both plastic and elastic stage decreased. It can be inferred that as for longitudinal ultrasonic vibration, the softening effect is the dominant mechanism, as for transversal ultrasonic vibration, the reduction in elongation and small softening effect is the dominant mechanism. However, whether this conclusion can be applied on other material remains further study. Detailed analysis can be found in **chapter 4.6**.

4.2 Ultrasonic vibration tension results of Copper 110

The ultrasonic vibration tension results of copper 110 shows a similar pattern as AA6061, the “small softening effect” was found in transversal ultrasonic tension test, and “distinct softening effect” can be seen in longitudinal tension test. Compared with tension results of AA6061, this similar pattern of copper 110 implying “small softening effect” (decrease in elongation under transversal UV) and “softening effect” (increase in elongation under longitudinal UV) is not individual case. **Figure 4.4** shows transversal ultrasonic tension result compared with static tension result of copper 110 and **Figure 4.5**

shows the effect of longitudinal ultrasonic tension result. Detailed analysis and comparison is in **chapter 4.6**.

4.3 Ultrasonic vibration tension results of AA1100

As for AA1100, similar pattern has been found under both transversal and longitudinal ultrasonic tension test results (shown respectively in **Figure 4.6** and **Figure 4.7**). However, the elongation in longitudinal ultrasonic tension test result is not as obvious as AA6061. Detailed analysis and comparison is in **chapter 4.6**.

4.4 Ultrasonic vibration tension results of Brass 260

Figure 4.8 and **Figure 4.9** exhibit the ultrasonic tension results of brass 260 (respectively transverse and longitudinal direction of UV). The pattern remains the same, whereas the decrease and increase in elongation were not apparent as found in AA6061 and Copper 110. Especially in longitudinal ultrasonic tension result, the strain is close to static tension result (longitudinal ultrasonic tension test still has larger elongation).

4.5 Ultrasonic vibration tension results of AA5086

Compare with brass 260, AA5086 has similar tension pattern in elongation, though longitudinal tension test exhibits larger elongation, the strain is close to static tension

result. The stress-strain curve of AA5086 ultrasonic tension results are shown in **Figure 4.10** and **Figure 4.11**.

4.6 Parameter identification of tension test

The parameters for transverse and longitudinal ultrasonic vibration conditions were calibrated and shown in this section; a comparison between transverse and longitudinal ultrasonic vibration tension test results indicates the properties of each condition.

4.6.1 Parameter identification of AA6061, Copper 110 and AA1100

According to Dieter[3], modulus of elasticity, ultimate tensile strength and strain at fracture point are among the most important parameters to characterize the mechanical properties of materials (besides there is ductility, tensile toughness, and will be discussed in **Chapter 5**). **Table 4.1** shows important parameters of AA6061, Copper and AA1100 (ductile metals) under two ultrasonic vibrations comparing with static tension force and their consistency are illustrated by standard deviations in parentheses.

Standard deviations were determined by,

$$\boldsymbol{\sigma} = \sqrt{\frac{\mathbf{1}}{\boldsymbol{N}} \sum_{\boldsymbol{i-1}}^{\boldsymbol{N}} (\boldsymbol{x_i} - \boldsymbol{\mu})^{\mathbf{2}}} \qquad (4\text{-}1)$$

Where $\boldsymbol{\mu}$ is mathematic expectation, $\boldsymbol{x_i}$ is one sample value, N, the total number of samples.

Figure 4.12 shows the comparison of elongation for AA6061, AA1100 and Copper 110 in column graph, the elongation reduces significantly when ultrasonic vibration is transversal (respectively 6.0%, 6.6% and 8.8%), and elongated when ultrasonic vibration is longitudinal (respectively 7.8%, 3.1% and 3.0%).

Figure 4.13 shows the comparison of ultimate tensile strength of AA6061, AA1100 and Copper 110 in column graph, the largest UTS of three materials happened in static tension test. More reduction of ultimate tensile strength under transversal ultrasonic vibration conditions (3.8% reduction for AA6061, 8.6% reduction for AA1100 and 5.5% reduction for Copper 110). And less reduction of UTS under longitudinal conditions (1.6% reduction for AA6061, 3.2% reduction for AA1100 and 2.2% reduction for Copper 110).

4.6.2 Parameter identification of AA5086 and Brass 260

Table 4.2 shows the important parameters of AA5086 and brass 260 of brittle metals (fractured soon after UTS), the effect of ultrasonic vibration was not as much as it in ductile metals, especially in strain. However, the trend remains the same, as shown in **Figure 4.14**, **Figure 4.14** shows the comparison of elongation AA5086 and Brass 260 in column graph, the elongation slightly reduces when ultrasonic vibration is transversal (respectively 3.7% and 3.8%), and elongated when ultrasonic vibration is longitudinal (respectively 3.4% and 1.3%).

Figure 4.15 shows the comparison of ultimate tensile strength of AA5086 and brass 260 in column graph, the largest UTS of three materials happened in static tension test. The reduction of ultimate tensile strength under transversal and longitudinal ultrasonic vibration conditions were very close (under transversal UV: 5.1% reduction for AA5086, 2.1% reduction for brass 260) (under longitudinal UV: 5.3% reduction for AA5086, 2.6% reduction for brass 260).

Table 4.1 Data of modulus of elasticity, UTS, strain at fracture point from ultrasonic/static tension tests of AA6061, AA1100, Copper 110. Standard deviation is given in parentheses.

Alloy	Modulus of elasticity (GPa)	UTS (MPa)	Strain at fracture point
	Transverse UV		
AA6061	72.6 (0.76)	296.23 (2.41)	0.204 (0.008)
AA1100	20.78 (1.65)	72.27 (1.43)	0.366 (0.011)
Copper 110	40.71 (2.81)	189.87 (3.84)	0.718 (0.023)
	Longitudinal UV		
AA6061	50.4 (1.42)	302.84 (2.78)	0.234 (0.015)
AA1100	61.31 (1.48)	76.51 (2.61)	0.404 (0.024)
Copper 110	13.47 (1.12)	196.58 (2.54)	0.811 (0.023)
	Static tension test		
AA6061	65.6 (0.87)	307.86 (3.14)	0.217 (0.009)
AA1100	106.64 (2.89)	79.10 (1.62)	0.392 (0.018)
Copper 110	64.52 (3.51)	200.98 (3.54)	0.787 (0.027)

Table 4.2 Data of modulus of elasticity, UTS, strain at fracture point from ultrasonic/static tension tests of AA5086 and Brass 260. Standard deviation is given in parentheses.

Alloy	Modulus of elasticity (GPa)	UTS (MPa)	Strain at fracture point
	Transverse UV		
AA5086	75.09 (1.78)	255.25 (2.97)	0.256 (0.007)
Brass 260	53.81 (2.36)	302.82 (3.41)	0.638 (0.018)
	Longitudinal UV		
AA5086	87.27 (1.77)	254.63 (3.41)	0.275 (0.024)
Brass 260	94.77 (0.94)	301.34 (2.88)	0.672 (0.012)
	Static tension test		
AA5086	103.03 (1.71)	268.91 (2.13)	0.266 (0.030)
Brass 260	104.48 (1.56)	309.43 (1.97)	0.663 (0.014)

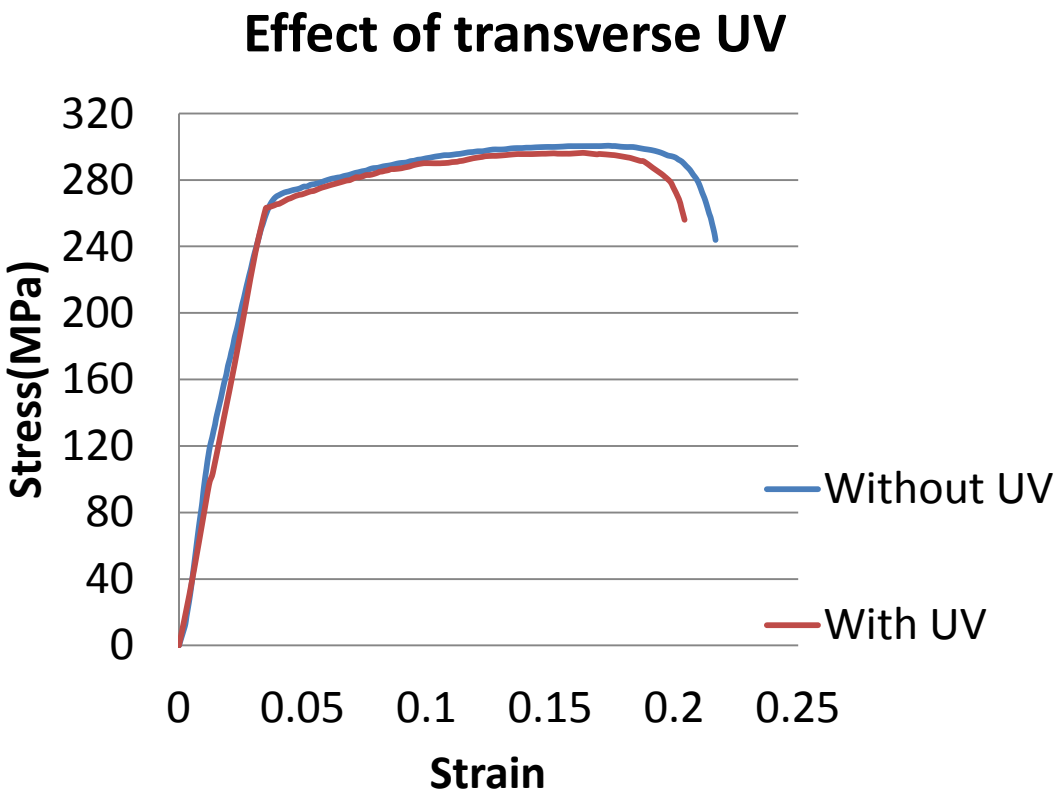

Figure 4.1 Stress-strain curves of AA6061 under static tension and transversal ultrasonic vibration.

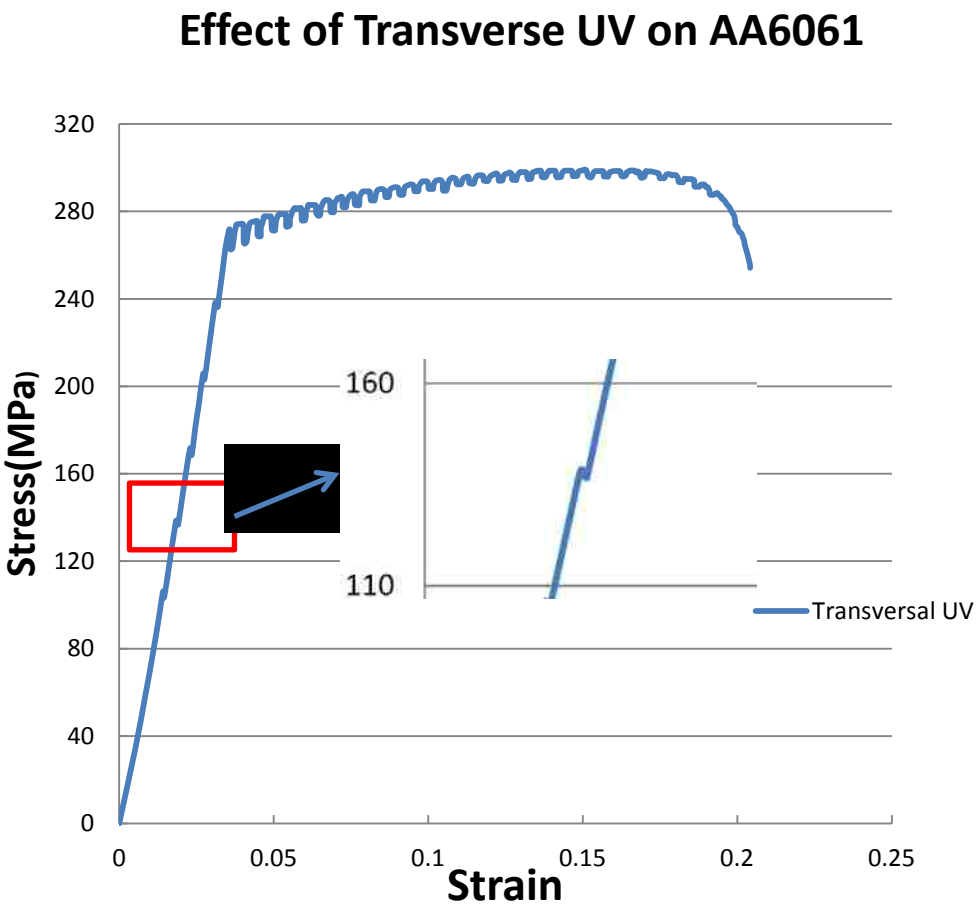

Figure 4.2 Stress-strain curves of AA6061 under intermittent transversal ultrasonic vibration, immediate stress reduction observed when transversal ultrasonic vibration was imposed.

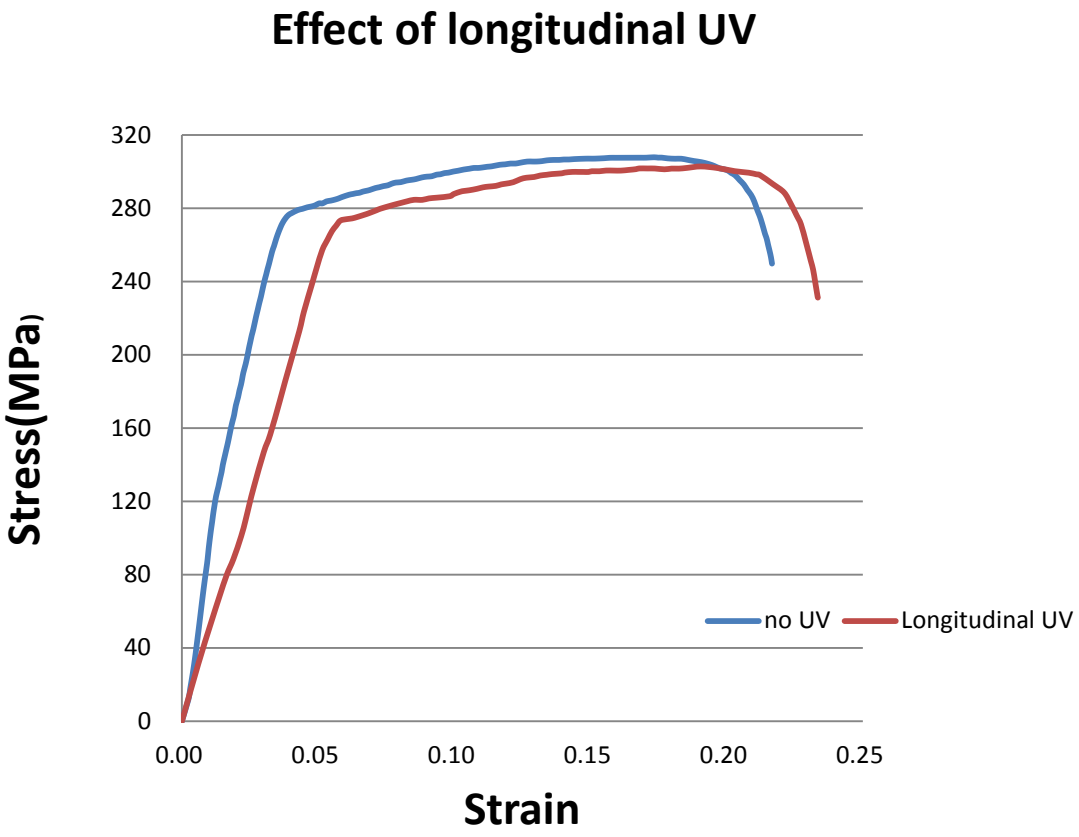

Figure 4.3 Stress-strain curves of AA6061 under static tension and longitudinal ultrasonic vibration.

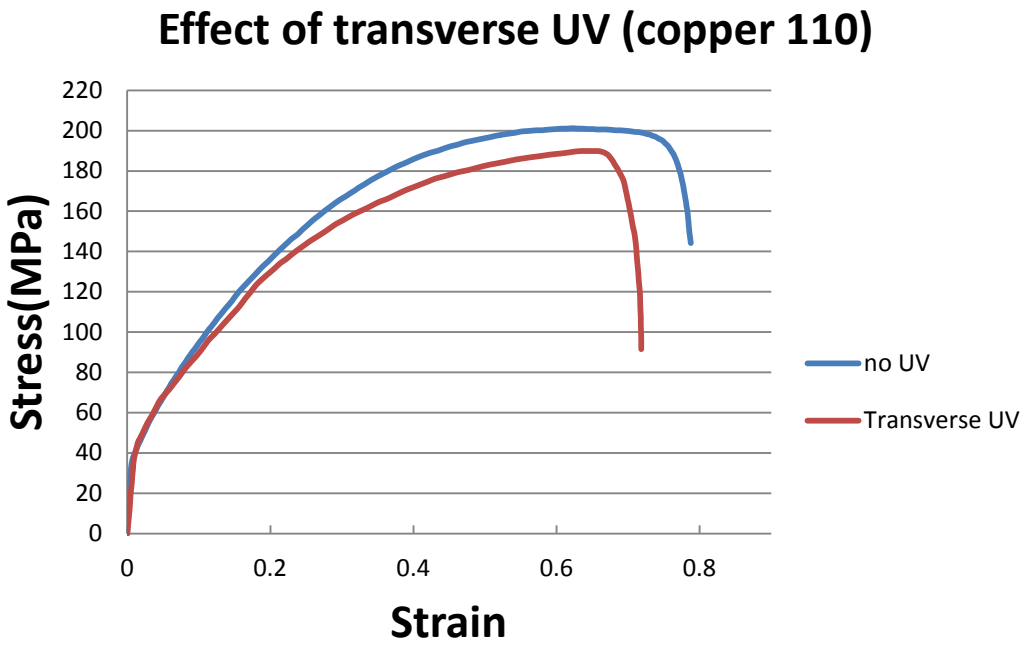

Figure 4.4 Stress-strain curves of copper 110 under static tension and transversal ultrasonic vibration.

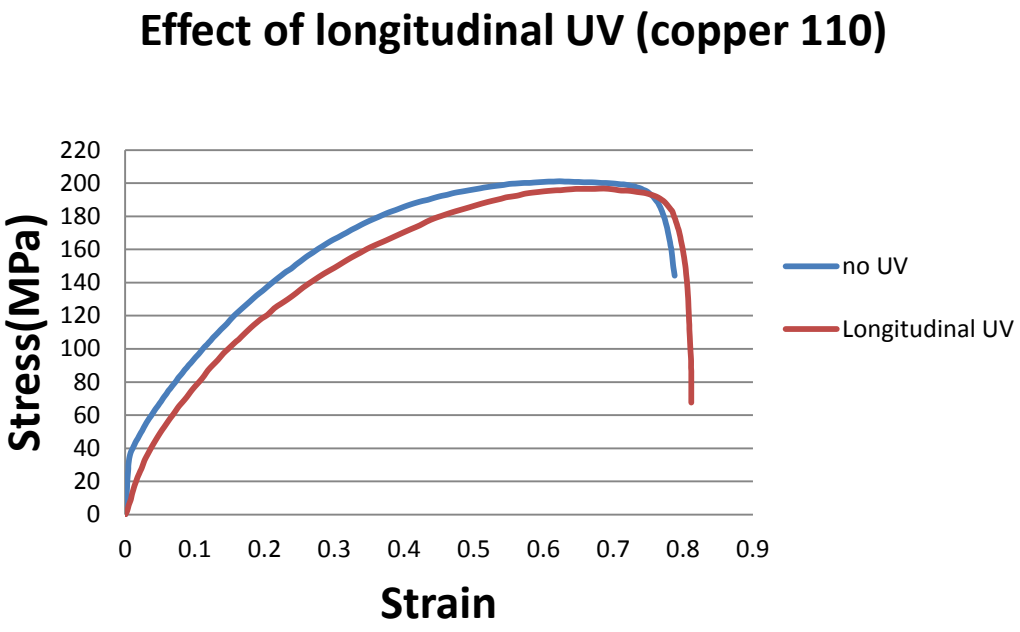

Figure 4.5 Stress-strain curves of copper 110 under static tension and longitudinal ultrasonic vibration.

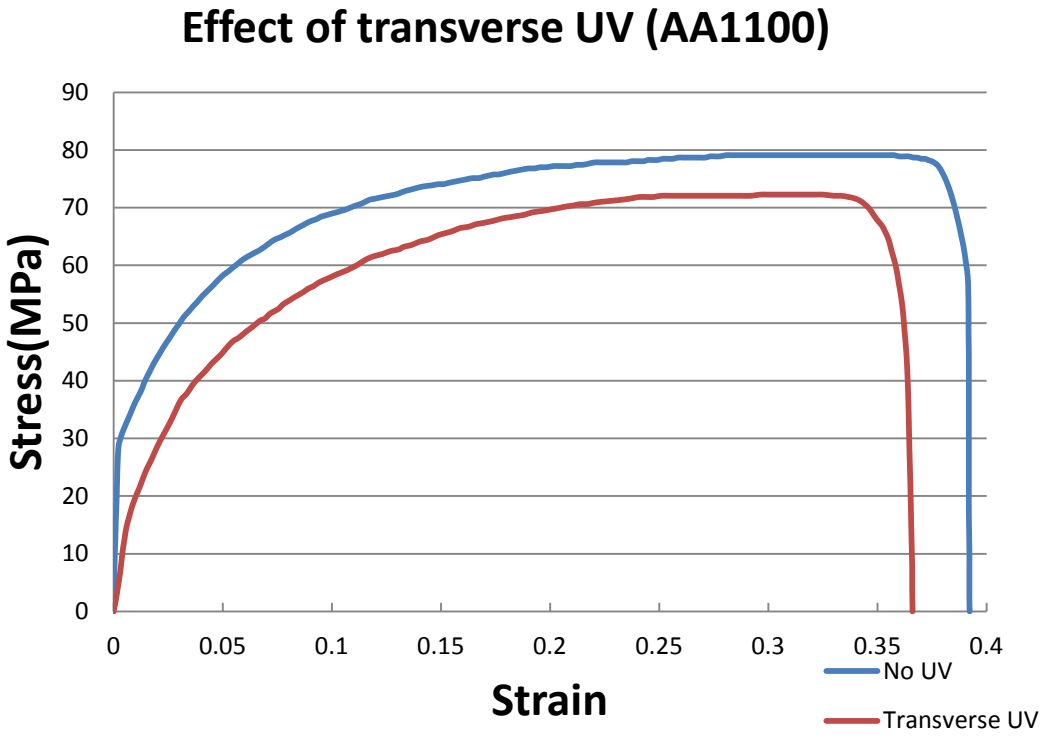

Figure 4.6 Stress-strain curves of AA1100 under static tension and transversal ultrasonic vibration.

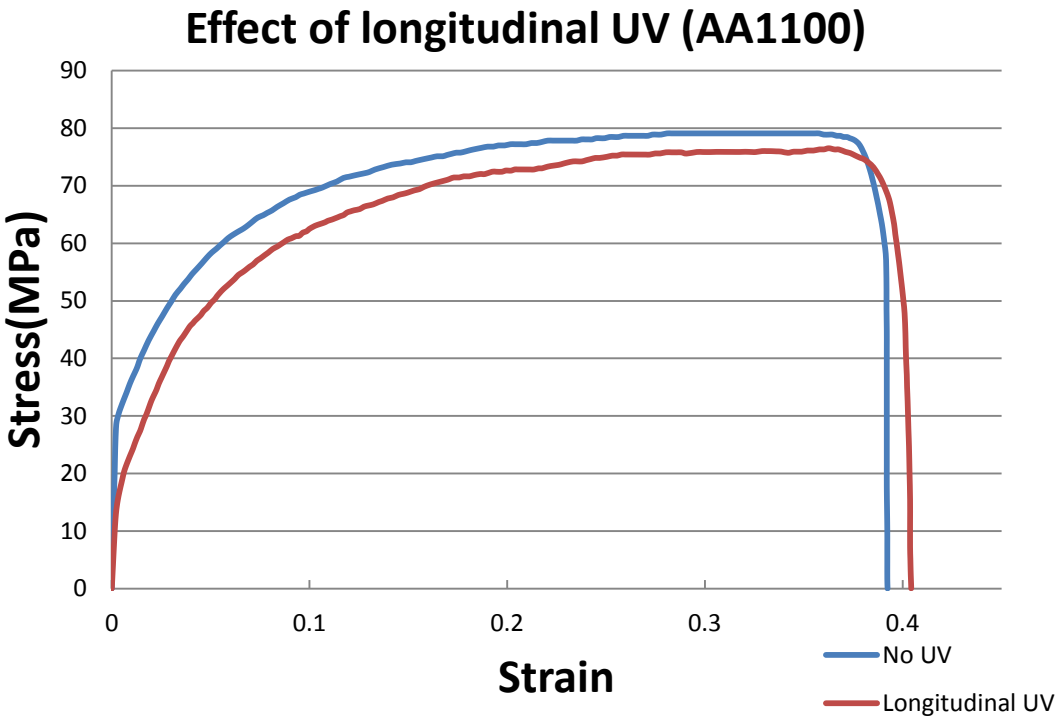

Figure 4.7 Stress-strain curves of AA1100 under static tension and longitudinal ultrasonic vibration.

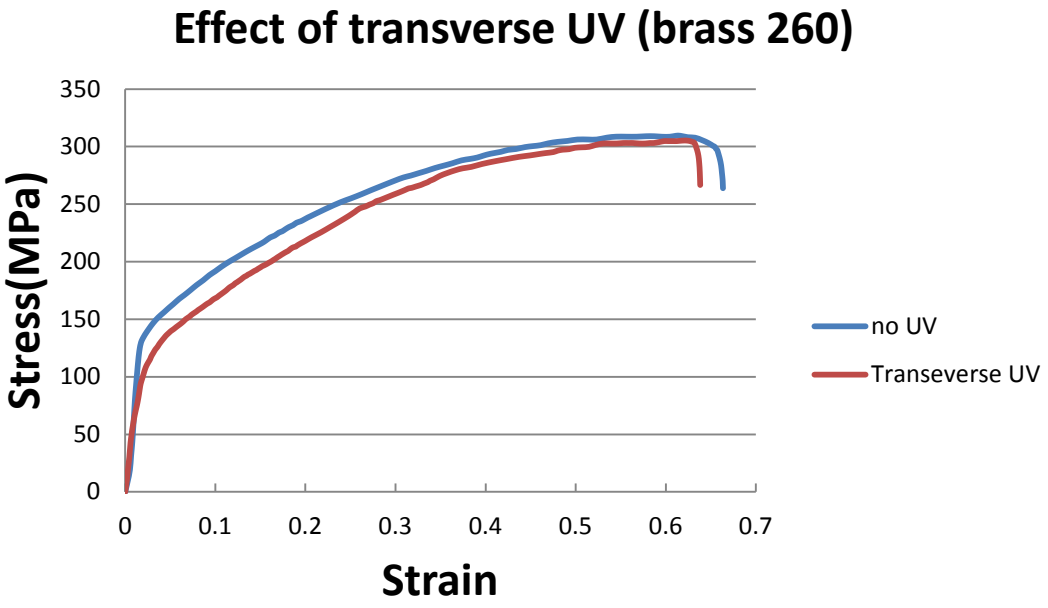

Figure 4.8 Stress-strain curves of Brass 260 under static tension and transversal ultrasonic vibration.

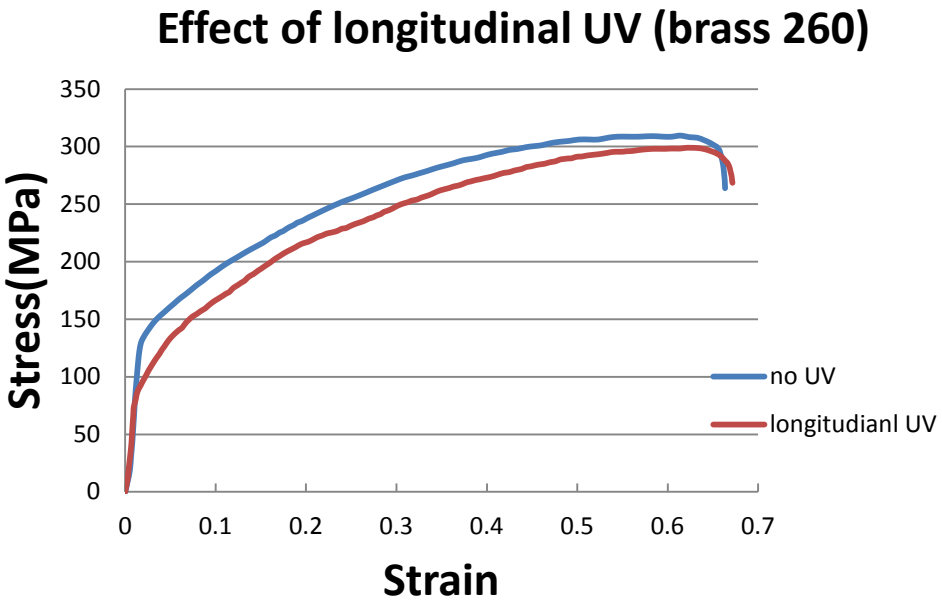

Figure 4.9 Stress-strain curves of Brass 260 under static tension and longitudinal ultrasonic vibration.

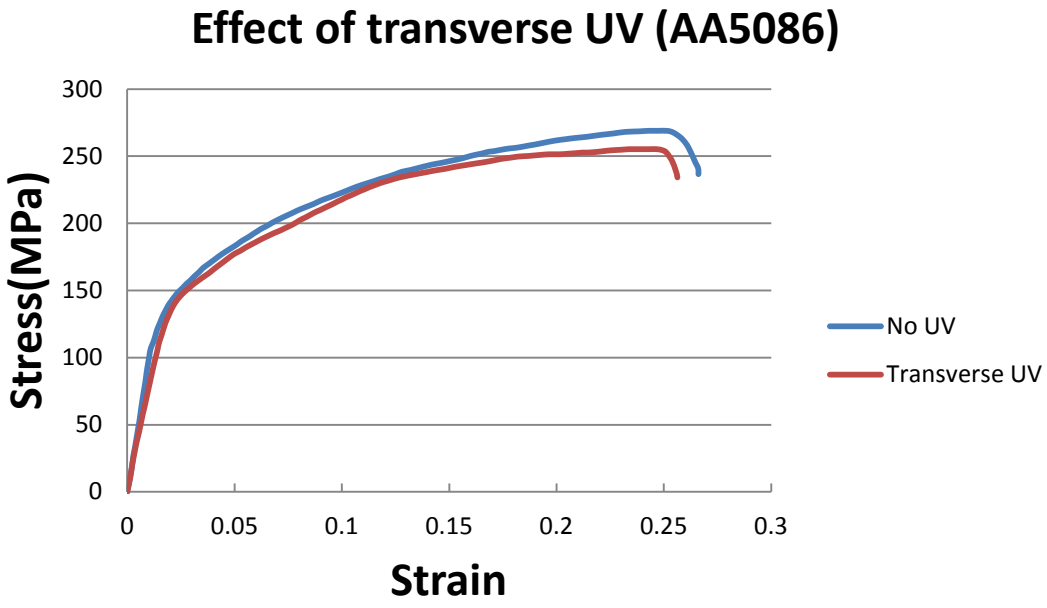

Figure 4.10 Stress-strain curves of AA5086 under static tension and transversal ultrasonic vibration.

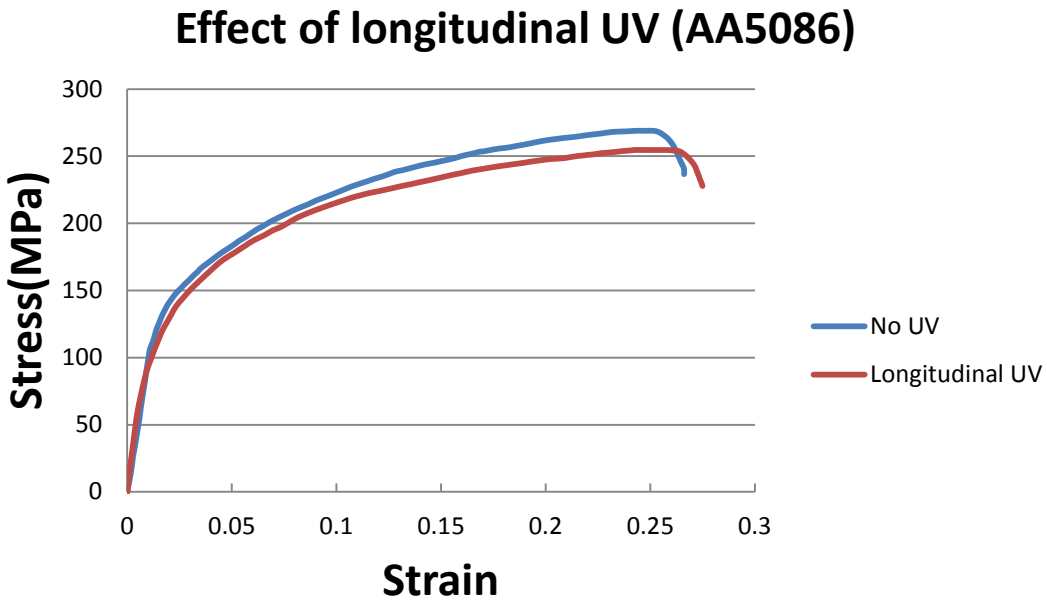

Figure 4.11 Stress-strain curves of AA5086 under static tension and longitudinal ultrasonic vibration.

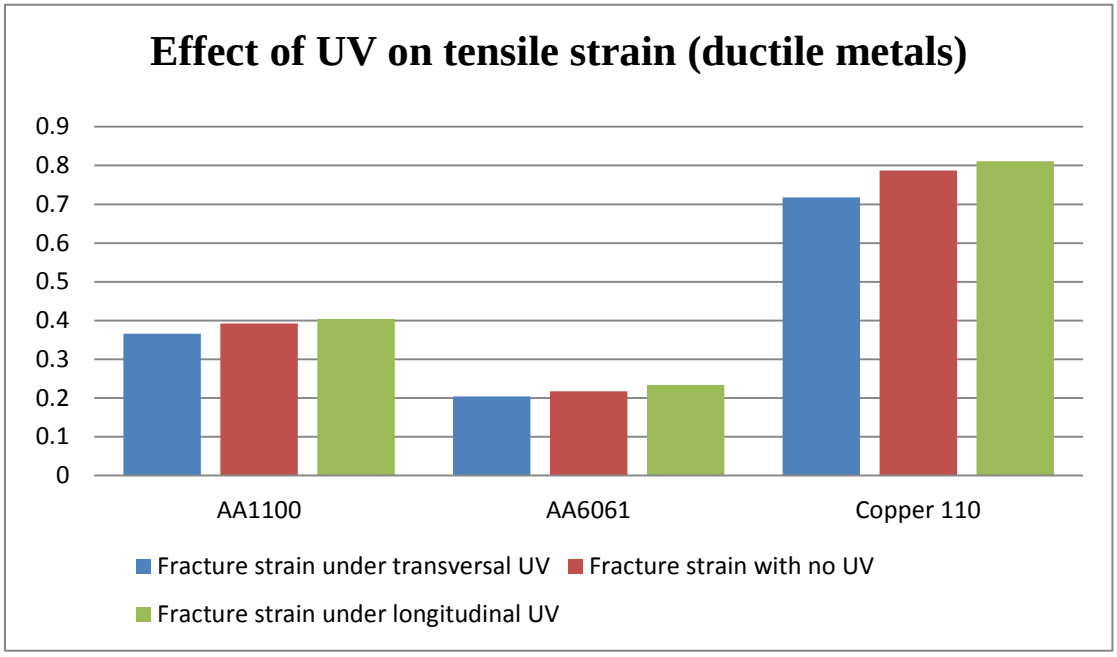

Figure 4.12 Maximum tensile strain at fracture point. Testing specimen: AA1100, AA6061 and Copper 110.

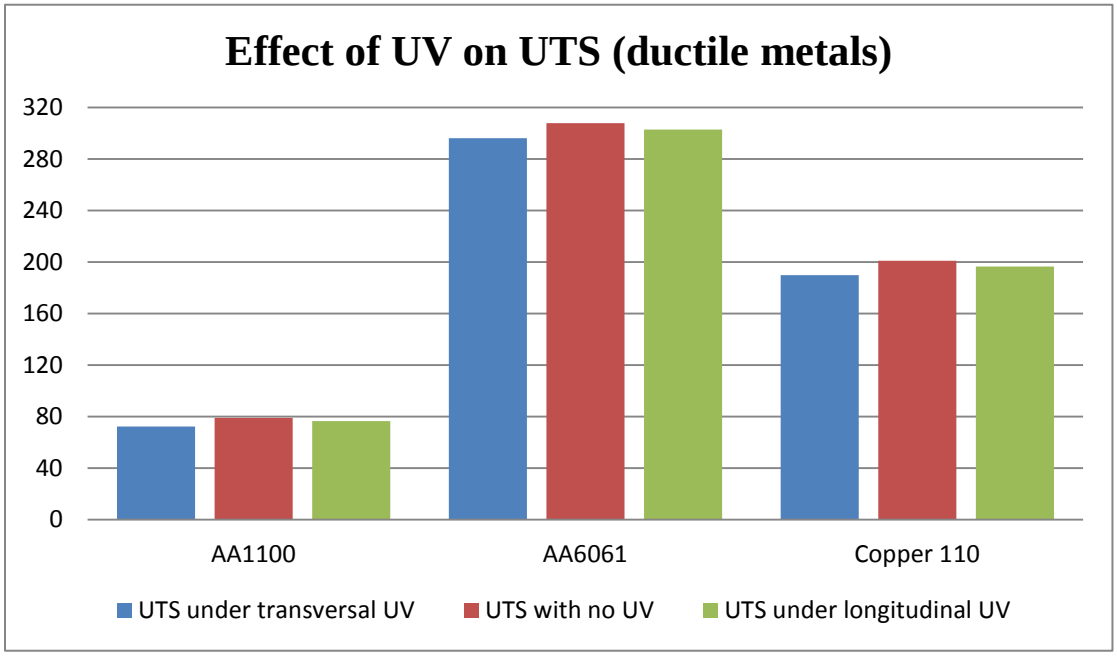

Figure 4.13 Ultimate tensile strength for three kinds of specimen: AA1100, AA6061 and Copper 110.

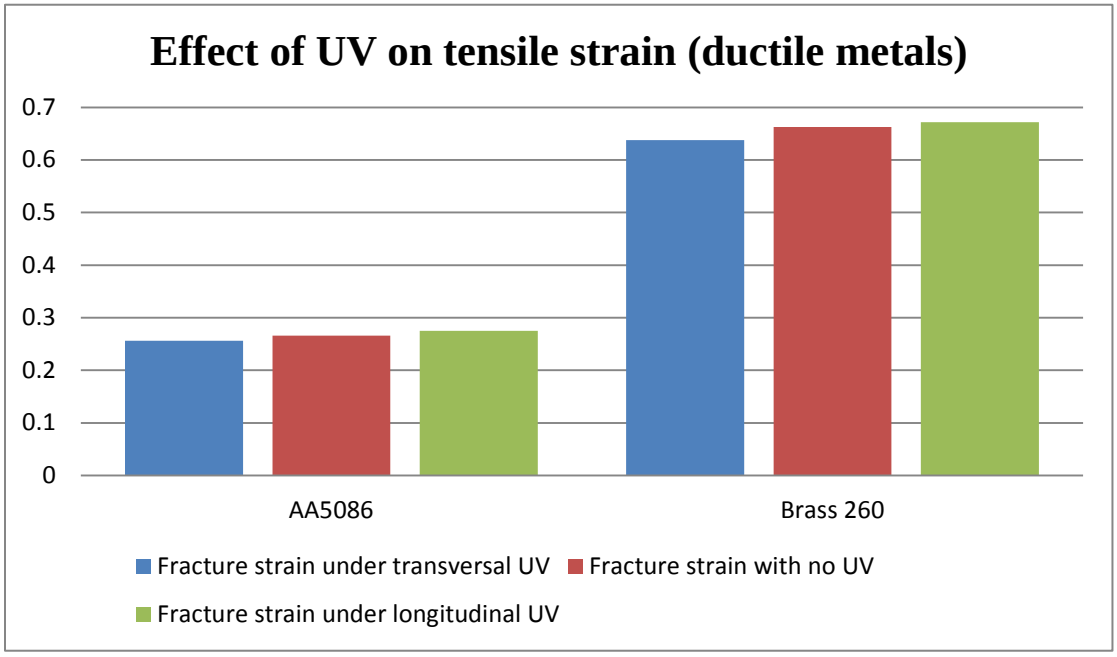

Figure 4.14 Maximum tensile strain at fracture point. Testing specimen: AA5086 and brass 260.

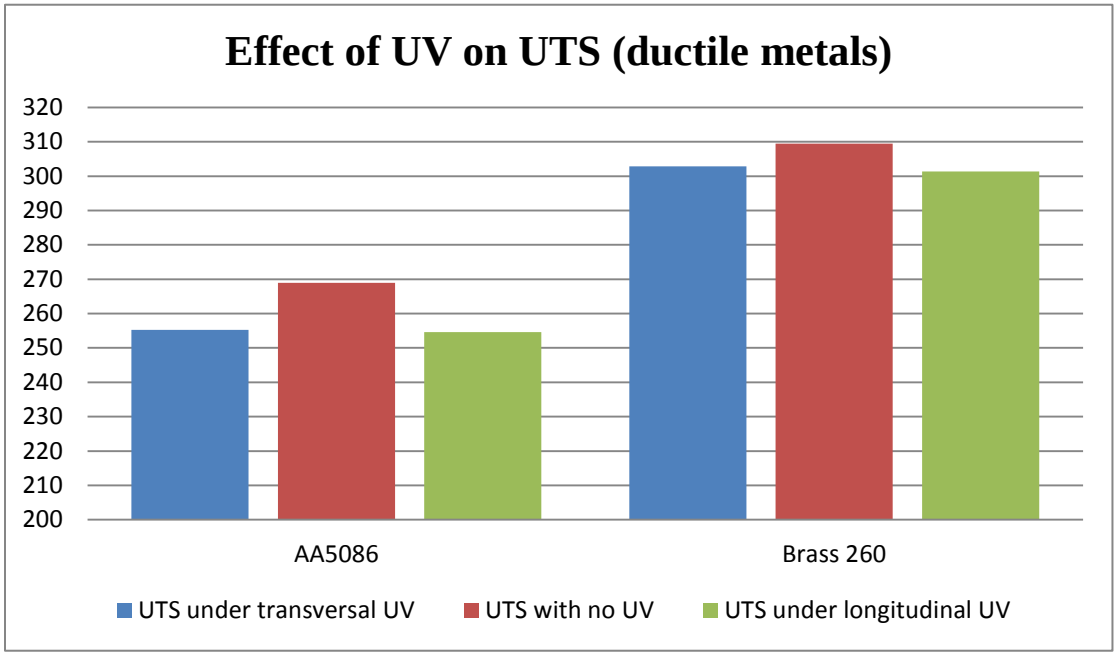

Figure 4.15 Ultimate tensile strength of AA5086 and brass 260.

Chapter 5: Discussions

5.1 Comparison of thermal energy and acoustic energy

In order to determine the source of stress reduction (no matter from transverse of longitudinal ultrasound), the energy density of ultrasonic wave is needed. According to the theory of wave energy [30], the wave energy-flux density (I) is proportional to the square of the amplitude (A) at a constant frequency (f), and gives:

$$\boldsymbol{I = \frac{P}{S} = \frac{1}{2}\rho A^2 \omega^2 u} \quad (5\text{-}1)$$

where P is the average energy flow (output power) through area S during a period of time, ρ is the density of the material that the ultrasonic can travel through (ρ=7.8×103 $kg/m3$ in steel), ω the angular velocity (ω=2πf), and u the wave velocity in the media (u=5200 m/s in steel). If P reaches the maximum power output of 700W and the energy loss is neglected, the estimated maximum amplitude (A) along the horizontal (or perpendicular to the tensile direction) is about 0.002 mm at the end of the sample.

It's been generally accepted that acoustic softening is an important source of stress reduction, though the mechanism of acoustic softening is still not so clear [31-37]. The factors causing the acoustic softening has been considered to be various elements, mainly used to attribute to thermal effects [38].

Although in this study, a clear breakthrough mechanism cannot be proposed, a macroscopic analysis can be performed to identify whether the stress reduction (acoustic

softening) is directed caused by elevated temperature in the process of ultrasonic vibration superimposing. Take AA6061 as an example:

Compare the thermal energy and ultrasonic energy to reduce the stress by 3.8% (under transverse ultrasonic vibration), AA6061 with ultrasonic energy: As shown in **Table 4.1**, the stress reduction is as large as 3.8% of the total stress, in order to achieve such extend stress reduction by pure heating, the temperature of the sample needs to increase to about $\mathbf{100}\ ℃$ according to the typical tensile property plotted at elevated temperatures in the ASM handbook[39].

Based on the heat density of the aluminum, to heat the aluminum sample from $\mathbf{25}$℃ **to** $\mathbf{100}$℃, the thermal density required is $\mathbf{1.9 \times 10^8 J/m^3}$. However, the applied acoustic energy density at the tip of ultrasonic transducer is around $\mathbf{85 J/m^3}$, based on the calculated vibration amplitude (Eq 5-2 by Hueter and Bolt 1955[40]).

$$\boldsymbol{w = \frac{1}{2}\rho A^2 \omega^2,\ where\ \omega = 2\pi f} \tag{5-2}$$

The comparison clearly shows the acoustic softening caused by ultrasonic wave is much more efficient than direct heating, and therefore, the elevated temperature during the ultrasonic wave superimposing cannot explain the whole mechanism.

5.2 The role of stress superposition in ultrasonic tension test

The stress superposition is a relatively abstract concept which can only be simulated by model (sometimes FE model [41]) due the lack of method to obtain real time data. As a

result, usually the mean flow stress (stable line in stress-strain curve) is taken as the result of effect of stress superposition (an oscillatory line), and this mean flow stress will be parallel with the static stress without ultrasonic vibration.

As can be seen in **Figure 5.1**, in elastic stage of stress-strain curve of AA6061 under transverse ultrasonic vibration, two are not parallel to each other (red line represents the path of stress under UV, black line represents the path of static stress), while in plastic deformation stage, although stress first increase and then decrease when pass UTS, two lines parallel to each other for the whole stage of deformation. From above, it can be deduced that the stress superposition happened mainly in the plastic stage of the metal forming process, and it is not the main mechanism of stress reduction in elastic stage, which is easy to be imagined, when the resistance of material continuous increase in elastic stage, oscillatory forces is hard to take in effect and can only be effective when the resistance of material and external load reach at a balance in plastic stage.

5.3 Effect of ultrasonic vibration from energy perspective

The ability to absorb energy when material withstands stresses above yield stress without fracturing is called tensile toughness. The area under stress-strain curve represents the amount of work per volume and therefore can be the value of tensile toughness. Elongation represents the formability of materials; more elongation (strain) means higher formability of material and increases its tensile toughness. In mass

production of metal forming, the ultimate goal is to form metals at lower stress with lower temperature, and at the mean time the formability of metal still can be retained.

In order to determine the effect of ultrasonic vibration, the tensile toughness of three conditions should be compared (transverse/ longitudinal UV and static tension). The method to calculate the area under the stress-strain curve is by integration using:

$$\int_0^b f(x)\,dx \tag{5-3}$$

Where $f(x)$ in the function that stress-strain curve represents, b is the strain at fracture point. Stress strain curves were intercepted until ultimate tensile strength since workpiece began to fail after this point.

For AA1100, as can be seen from **Figure 5.2**, the comparison between transverse and longitudinal UV, the tensile toughness of two ultrasonic vibration conditions are respectively $18.7 \times 10^6\ J/m^3$ and $23.6 \times 10^6\ J/m^3$, and for static tension test, the value is $22.2 \times 10^6\ J/m^3$.

For AA5086, **Figure 5.3** shows the comparison between transverse and longitudinal UV, the tensile toughness under longitudinal ultrasonic vibration is $53.3 \times 10^6\ J/m^3$, for transverse ultrasonic vibration, the tensile toughness is $52.0 \times 10^6\ J/m^3$, and for static tension test, the value is $52.8 \times 10^6\ J/m^3$.

For AA6061, as can be seen from **Figure 5.4**, the comparison between transverse and longitudinal UV, the tensile toughness under longitudinal UV is $47.0 \times 10^6\ J/m^3$,

the tensile toughness under transverse UV is $\mathbf{41.5 \times 10^6\ J/m^3}$. For static tension test, the tensile toughness is $\mathbf{46.3 \times 10^6\ J/m^3}$.

For brass 260, **Figure 5.5** shows the comparison between transverse and longitudinal UV, the tensile toughness under longitudinal ultrasonic vibration is $\mathbf{147.5 \times 10^6\ J/m^3}$, for transverse ultrasonic vibration, the tensile toughness is $\mathbf{139.5 \times 10^6\ J/m^3}$, and for static tension test, the value is $\mathbf{154.2 \times 10^6\ J/m^3}$.

For copper 110, as can be seen from **Figure 5.6**, the comparison between transverse and longitudinal UV, the tensile toughness under longitudinal UV is $\mathbf{91.5 \times 10^6\ J/m^3}$, the tensile toughness under transverse UV is $\mathbf{91.0 \times 10^6\ J/m^3}$. For static tension test, the tensile toughness is $\mathbf{94.6 \times 10^6\ J/m^3}$.

By summarizing the data above, it can be concluded that:

1. The tensile toughness value from longitudinal UV and static tension test are close, tensile toughness under transverse UV is the lowest among three conditions.
2. The reason of close tensile toughness value between longitudinal UV and static tension test is because more elongation happened in longitudinal tension test (the formability of metal becomes better under longitudinal UV).
3. Two strategies are provided: i) if the priority in production is less energy consumption, transverse ultrasonic UV should be a better option. ii) if more

deformability is most wanted in metal forming process, longitudinal UV has its advantage.

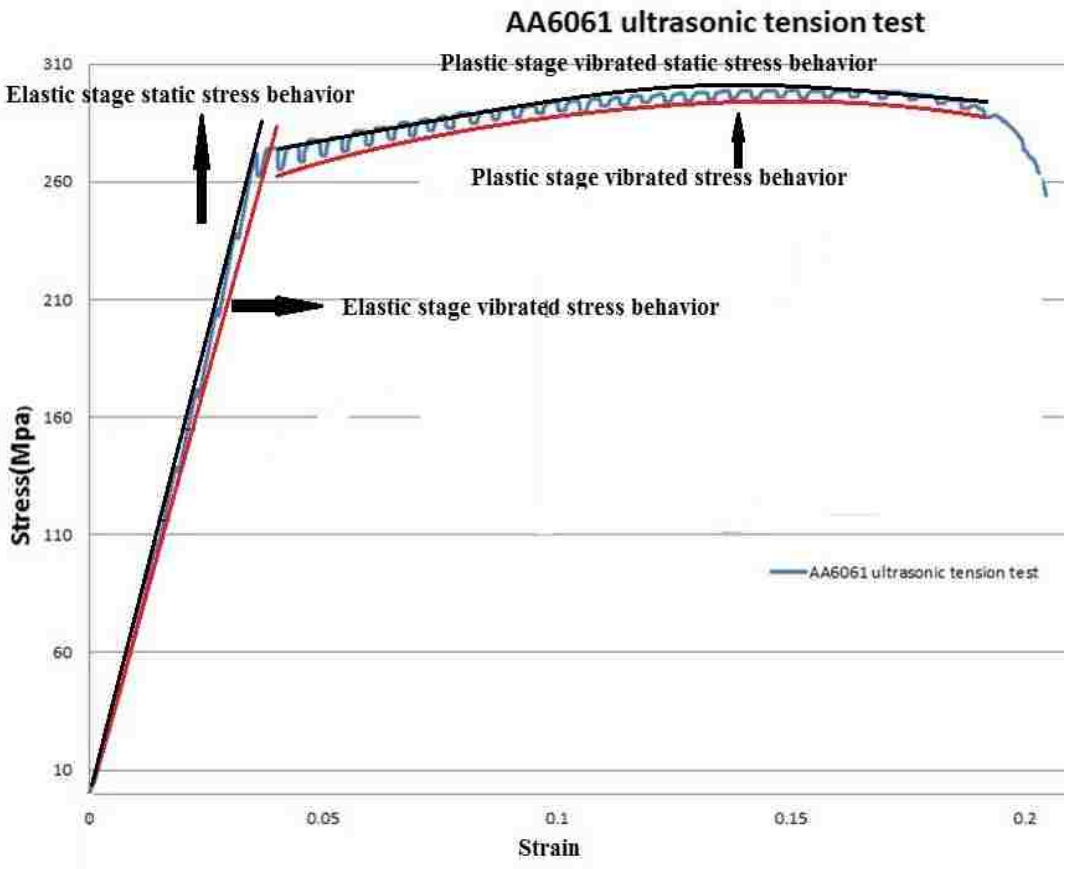

Figure 5.1 Effect of stress superposition in elastic/plastic stage of transversal ultrasonic vibration tension test of AA6061.

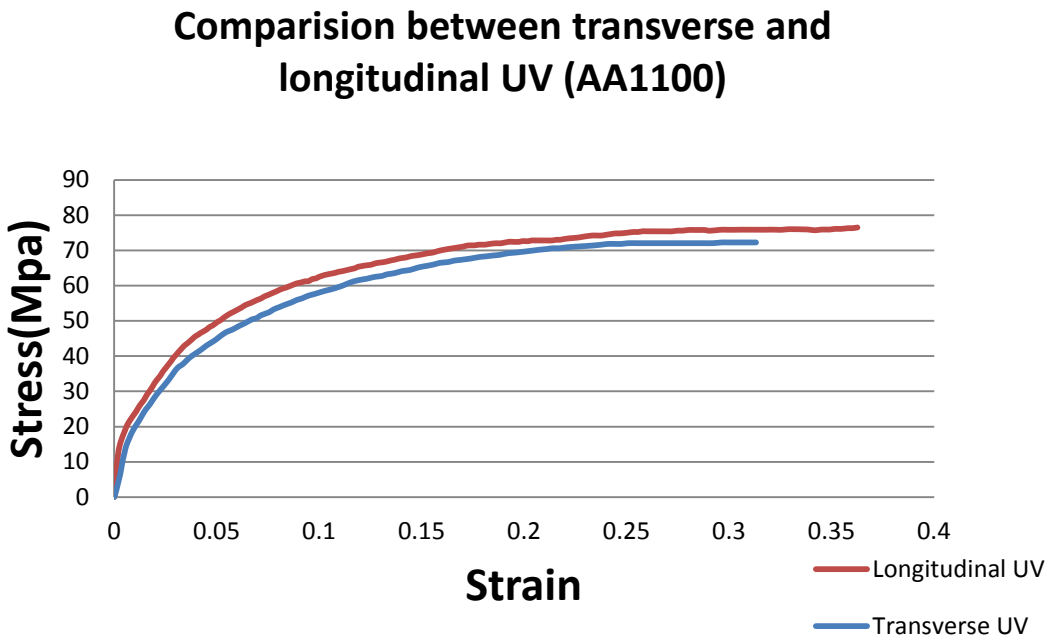

Figure 5.2 The comparison between transverse and longitudinal ultrasonic vibration of AA1100, the stress-strain is intercepted until ultimate tensile strength.

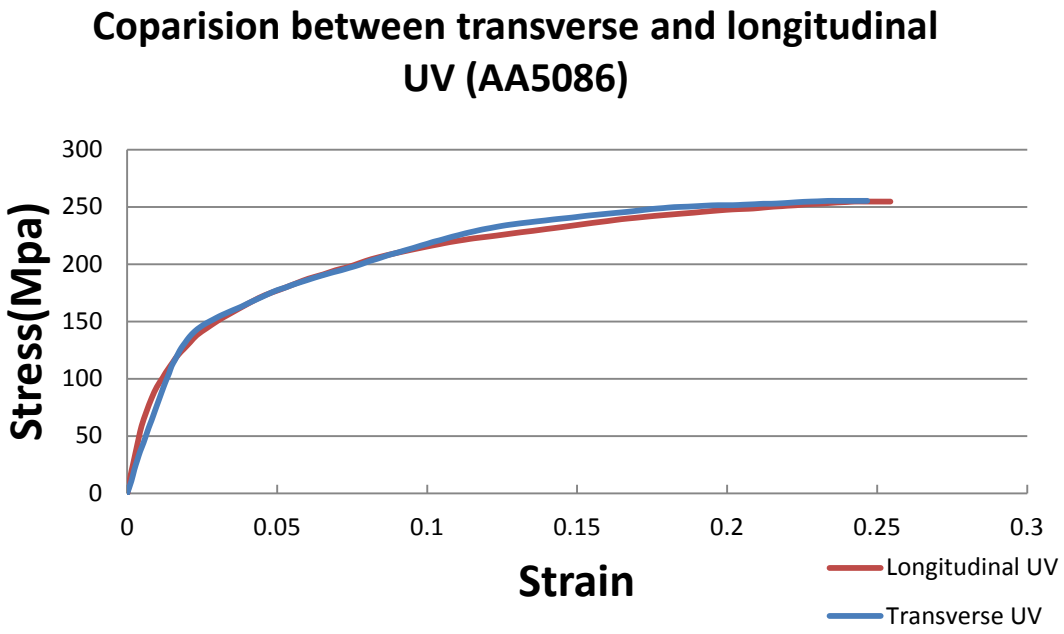

Figure 5.3 The comparison between transverse and longitudinal ultrasonic vibration of AA5086, the stress-strain is intercepted until ultimate tensile strength.

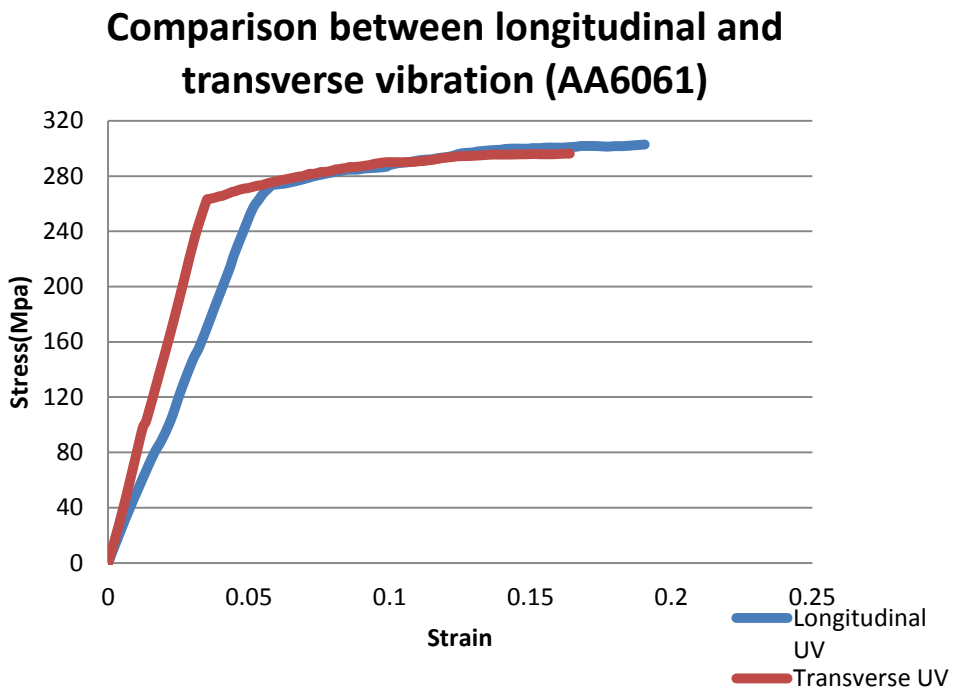

Figure 5.4 The comparison between transverse and longitudinal ultrasonic vibration of AA6061, the stress-strain is intercepted until ultimate tensile strength.

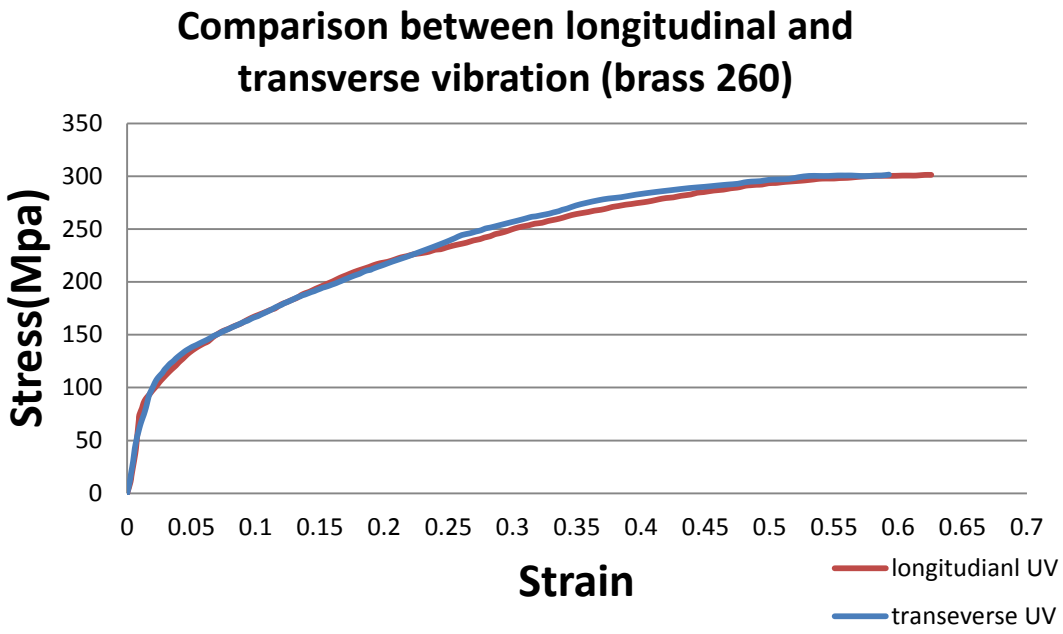

Figure 5.5 The comparison between transverse and longitudinal ultrasonic vibration of Brass 260, the stress-strain is intercepted until ultimate tensile strength.

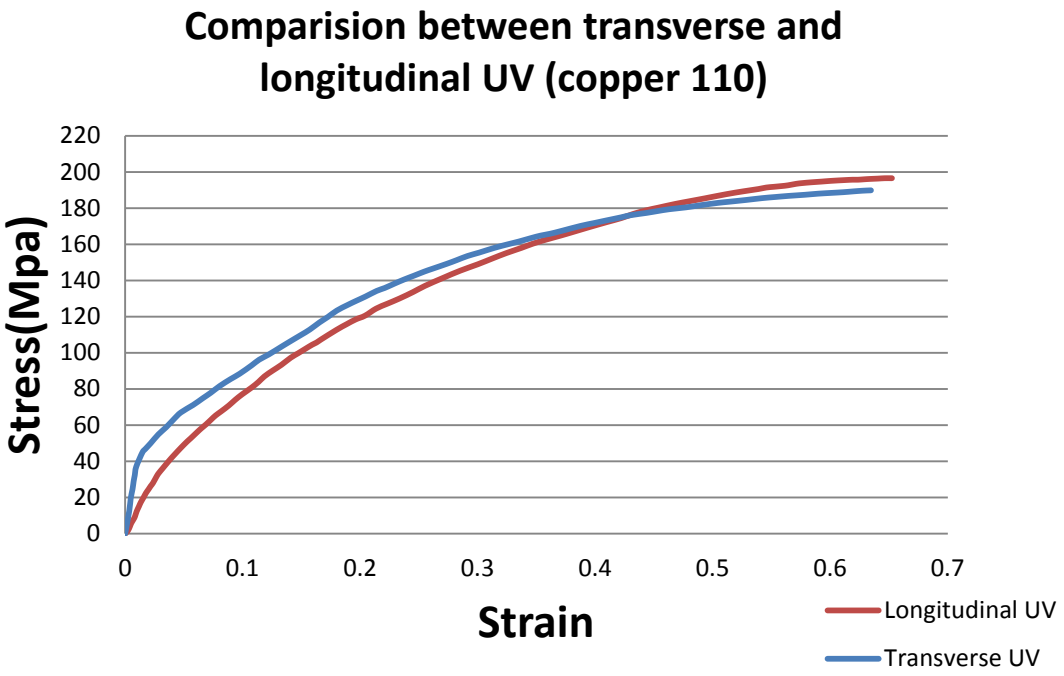

Figure 5.6 The comparison between transverse and longitudinal ultrasonic vibration of Copper 110, the stress-strain is intercepted until ultimate tensile strength.

Chapter 6: Conclusions

6.1 Conclusions

In this research the effect of superposition of ultrasonic wave on stress and strain during tension test of AA6061, AA5086, AA1100, Brass 260 and Copper 110 was studied. The main conclusions are as follows:

1) For all five metals (AA6061, AA5086, AA1100, Brass 260 and Copper 110), transversal ultrasonic vibration tends to reduce their strain at fracture, while longitudinal ultrasonic vibration tends to increase the strain at fracture.

2) No matter under transversal or longitudinal ultrasonic vibration, the flow stress is reduced by its effect: under transversal UV, the ultimate tensile strength is reduced by 3.8% for AA6061, 8.6% for AA1100, 5.5% for Copper 110, 5.1% for AA5086, 2.1% for brass 260; under longitudinal UV, the ultimate tensile strength is reduced by 1.6% for AA6061, 3.2% for AA1100, 2.2% for Copper 110, 5.3% for AA5086, 2.6% for brass 260. Generally, more flow stress reduction happened under transversal ultrasonic vibration compared with longitudinal ultrasonic vibration.

3) From comparison between direct heat and acoustic vibration, to obtain the same amount of flow stress reduction, ultrasonic vibration is a much more efficient way.

6.2 Future work

Because of the complexity of ultrasonic vibration within workpieces and the effect of ultrasonic vibration on microscopic level of deforming material remains unclear. Further research should be focused on:

1) The deformation process is sensitive to the change of amplitude of vibration; different power of ultrasonic transducer must be applied in order to discover the mechanisms.
2) To understand the changes in the microscopic scale of materials when experiencing ultrasonic deforming process.

REFERENCES

1. E. Ghassemali, X. Son, M. Zarinejad, D. Atsushi, M, Tan, Bulk Metal Forming Processes in Manufacturing. In A. Nee (Ed.), Handbook of Manufacturing Engineering and Technology, 2014, pp15, 18.
2. K. Lange, L. Cser, M. Geiger, J.A.G. Kals, Tool Life and Tool Quality in Bulk Metal Forming, CIRP Annals - Manufacturing Technology, Volume 41, Issue 2, 1992, pp224-225.
3. G. E. Dieter, Mechanical Metallurgy. 3rd ed., McGraw-Hill Book Co., New York 1986, pp 7-9,pp275-296.
4. ASTM, E8/E8M Standard Test Methods of Tension Testing of Metallic Materials, Annual Book or ASTM Standards, American Society for Testing and Materials, Vol. 3.01
5. S. Kalpakjian, S. Schmid, D. Design, Manufacturing, Engineering and Technology SI 6th Edition - Serope Kalpakjian and Stephen Schmid: Manufacturing, Engineering and Technology: Prentice Hall. 2006, pp65.
6. J. A. Gallego-Juárez, K. F. Graff, Power Ultrasonics. Oxford: Woodhead Publishing. 2015, pp144-147.
7. D. R. Culp, H.T. Gencsoy, Metal deformation with ultrasound, Ultrason. Symp, 1973, pp195.

8. B. Langenecker, W. H. Frandsen, S. R. Colberg, Kinking in zinc crystals by ultrasonic waves, J. Inst. Metals, vol. 91, No. 71, 1963, pp316-317.
9. E.A. Eaves, A.W. Smith, W.J. Waterhouse, D.H. Sansome, Review of the application of ultrasonic vibrations to deforming metals, Ultrasonics 13, 1975, pp162-170.
10. I. Kristoffy, Metal forming with vibrated tools, Trans. ASME J. Eng. Ind., 1969, pp1168-1174.
11. C.E. Winsper, G.R. Dawson, D.H. Sansome, An introduction to the mechanics of oscillatory metalworking, Met. Mater, 1970, pp158-162.
12. O. Izumi, K. Oyama, Y. Suzuki, On the superimposing of ultrasonic vibration during compressive deformation of metals, Trans. Jpn. Inst. Met. 7, 1966, pp158-162.
13. F. Blaha, B. Langenecker, Dehnung von Zink-Kristallen unter Ultraschalleinwirkung, Naturwissenschaften, 42(20), 1955, pp556-556.
14. Z. Huang, M. Lucas, M. J. Adams, Viscoplastic material upsetting with oscillating dies, in: Proceedings of the SEM IX International Congress & Exposition on Experimental Mechanics, Orlando, USA, 2000, p. 434.
15. R. Pohlman, E. Lehfeldt, Influence of ultrasonic vibration on metallic friction, Ultrasonics, 1966, pp178.
16. T. Wen, C. L. Pei, C. K. Li, Application of vibration in plastic forming processes, Hot Work. Technol., 38, 2009, pp114.
17. Z. H. Huang, M. Lucas, M. J. Adams, Study of ultrasonic upsetting under radial and

longitudinal die vibration. Materials Science Forum 440–441, 2003, pp389-396.

18. A.T. Bozdana, N.N.Z. Gindy, H. Li, Deep cold rolling with ultrasonic vibrations—a new mechanical surface enhancement technique, Int. J. Mach. Tools Manuf., 45, 2005, pp713.
19. T. Wen, L. Wei, X. Chen, C. Pei, Effects of ultrasonic vibration on plastic deformation of AZ31 during the tensile process. International Journal of Minerals, Metallurgy, and Materials, 18(1), 2011, pp70-76.
20. Z. Yao, G. Y. Kim, L. Faidley, Q. Zou, D. Mei, Z. Chen, Effects of superimposed high-frequency vibration on deformation of aluminum in micro/meso-scale upsetting. Journal of Materials Processing Technology, 212(3), 2012, pp640-646.
21. R. Ebrahimi, A. Najafizadeh, A new method for evaluation of friction in bulk metal forming. Journal of Materials Processing Technology, 2004, pp136-143.
22. K. F. Ehmann, R. E. DeVor, S. G. Kapoor, Micro/meso-scale mechanical manufacturing – opportunities and challenges. In: JSME/ASME International Conference on Materials and Processing, Honolulu, HI, USA, 2002, pp6-13.
23. J. C. Hung, Y. C. Tsai, C. H. Hung, Frictional effect of ultrasonic-vibration on upsetting. Ultrasonics 46, 2007, pp277-284.
24. T. Jimma, Y. Kasuga, N. Iwaki, O. Miyazawa, E. Mori, K. Ito, H. Hatano, An application of ultrasonic vibration to the deep drawing process. Journal of Materials Processing Technology 80–81, 1998, pp406-412.

25. H. O. K. Kirchner, W. K. Kromp, F. B. Prinz, P. Trimmel, Plastic deformation under simultaneous and unidirectional loading at low and ultrasonic frequencies, Mater. Sci. Eng. 68, 1984–1985, pp197–206.
26. Y. Bai, M. Yang, Deformation analysis of brass in micro compression test with presence of ultrasonic vibration. International Journal of Precision Engineering and Manufacturing, 16(4), 2015, pp 685-691.
27. G. Behme, T. Hesjedal, Influence of surface acoustic waves on lateral forces in scanning force microscopies, Journal of Applied Physics 89 (9), 2001, pp4850.
28. Y. Daud, M. Lucas, Z. Huang, Superimposed ultrasonic oscillations in compression tests of aluminium. Ultrasonics, 44, 2006, pp.e511-e515.
29. B. Langenecker, Effects of ultrasound on deformation characteristics of metals. IEEE Transactions on Sonics and Ultrasonics 13, 1996, pp1-8.
30. Y.D. Zhang, Ultrasonic Machining and its Application, National Defense Industry Press, Beijing, 1995, p.17.
31. B. Schinke, T. Malmberg, Dynamic tensile tests with superimposed ultrasonic oscillations for stainless steel type 321 at room temperature. Nuclear Engineering and Design 100, 1987, pp281-296.
32. K. Siegert, A. Mock, R. Malek, S. Y. Oh, Flexible micro metal forming with ultrasonically oscillating dies. Production Engineering III, 1996, pp25-28.
33. G. Ngaile, C. Bunget, Influence of ultrasonic vibration on micro-extrusion.

Ultrasonics 51, 2011, pp 606-616.

34. A. G. Rozner, Effect of ultrasonic vibration on coefficient of friction during strip drawing. Journal of the Acoustical Society of America 49, 1997, pp1368-1371.
35. V. C. Kumar, M. Hutchmgs, Reduction of the sliding friction of metals by the application of longlludinal or transverse ultrasonic vibration, Tribology International , 2004 , 37 (10), pp833-840.
36. P. Schwaller, P. Groning, A. Schneuwly, Surface and friction characterization by thermoelectric measurements during ultrasonic frichon process, U1trasonics , 2000, 38(1), pp212 -214.
37. G. R. Dawson, C. E. Winsper, D. H. Sansome, Application of high-frequency and low-frequency oscillations to plastic deformation of metals. Part 2. A complete appraisal of the development and potential. Metal Forming 37,1970, pp 254-261.
38. O. Izumi, K. Oyama, Y. Suzuki, Y. Effects of superimposed ultrasonic vibration on compressive deformation of metals. Transactions of the Japan institute of metals, 7(3), 1966, pp162-167.
39. J. G. Kaufman, Properties of Aluminum Alloys: Tensile, Creep, and Fatigue Data at High and Low Temperatures. ASM International, Metals Park, Ohio. 1999, pp105.
40. T. F. Hueter, R. H. Bolt, R.H, Sonics: Techniques for the Use of Sound and Ultrasound in Engineering and Science. Wiley, New York. 1955, p42.
41. Y. Daud, M. Lucas, Z. Huang, Modelling the effects of superimposed ultrasonic

vibrations on tension and compression tests of aluminium. Journal of Materials Processing Technology, 186(1–3), 2007, pp179-190.

VITA AUCTORIS

NAME:	Chen Ye
PLACE OF BIRTH:	Beijing, China
YEAR OF BIRTH:	1990
EDUCATION:	China University of Geosciences, Beijing, China
	2009-2012; B.Sc.
	University of Windsor, Windsor, Ontario, Canada
	2013-2016; M.A.Sc.